A University of Sussex MPhil thesis

Available online via Sussex Research Online:

http://sro.sussex.ac.uk/

MECHANOCHEMICAL SYNTHESIS OF DIIMIDE BASED ELECTRON ACCEPTORS FOR ORGANIC PHOTOVOLTAICS APPLICATIONS

A thesis submitted in partial fulfilment of the requirements for the degree of

Master of Philosophy
in
Chemistry

by

Hugo EMERIT

23 February 2022

Department of Chemistry
School of Life Sciences
University of Sussex

STATEMENT

I hereby declare that this thesis has not been and will not be, submitted in whole or in part to another University for the award of any other degree.

Signature:

ABSTRACT

It has been predicted that solar energy will play a key role in solving the serious environmental problems that face our planet. The pursuit of clean, renewable, cost-effective, and high-performance organic photovoltaic (OPV) technologies has attracted considerable efforts from both academia and industry. Some of the most promising materials for OPVs are those based on systems such as naphthalene diimide (NDI), or perylene diimide (PDI). These structures are known to be excellent electron acceptor species for organic electronic applications because of their strong light absorption and chemical stability. However, the efficient synthesis of these compounds is hindered by poor yields and the need for harsh solvent-based conditions, especially for their brominated derivatives. This report details our efforts towards synthesising these high value compounds in a more environmentally friendly way using solvent free mechanochemistry in a ball mill. With these molecules synthesised, our long-term goal is to study their solid-state polymerisation resulting in an environmentally benign synthesis of materials suitable for the next generation of organic solar cells.

ACKNOWLEDGEMENTS

I would like to take this opportunity to thank all the people who have contributed in some way to this thesis.

First and foremost, I am extremely grateful to my supervisor Dr Barnaby Greenland, for his guidance, and for his constant positiveness. I truly was impressed by the way he could always find a little positivity about anything, in any situation, or that any idea was good to consider. Today, his state of mind remains an example for me. I also won't forget his continuous availability when I needed professional or personal support. I can now say, without a doubt, that Barny has been the best mentor I had the opportunity to work with, during all these years studying chemistry.

Secondly, I wish to sincerely thank Sergi Ortoll, because this journey would not have been the same without him. Even in difficult times, I knew he was the one I could confide in and talk to about anything. Every minute spent with him was enjoyable: at the lunchroom first, trying to get along with anybody; at the lab, listening to French and Spanish songs; or at the pub, drinking tasty English beers in front of a good football game. I can easily say that he was like a second brother back there, and I hope we can maintain this friendship as long as possible.

I am also deeply grateful to Lydia Pearce for exploiting the best of my results, and for the writing of the first research article[1] that will leave a positive mark of my work on the international science community. Thanks to her and to Mary Wong, Arathy Jose, and Raysa Khan, for their invaluable advice and help on many occasions. Working along such lovely people was a real pleasure. From the beginning to the end, I could always count on the four of them. I have no doubt that the future of women in science is in good hands thanks to brilliant chemists like them.

Then, I want to acknowledge Pr Mark Bagley and all the members of the chemistry department, from the undergrad students to the lecturers. All the help received by any of them has been truly appreciated, especially at the beginning, when I had to make my marks at the university. For some of them, I am proud to have been their mechanochemistry initiator. During those moments, and for the first time in my life, I felt like I was a decent chemist.

TABLE OF CONTENTS

DETAILED TABLE OF CONTENTS

TABLE OF FIGURES

ABBREVIATIONS

OPV	organic photovoltaic
OSC	organic solar cell
NDI	naphthalene diimide
PDI	perylene diimide
PMDI	pyromellitic diimide
NDA	naphthalene-2,3-dicarboxaldehyde
IUPAC	International Union of Pure and Applied Chemistry
MM	VBM
VMB	vibratory ball mill
TSE	twin-screw extruder
PBM	planetary ball mill
DMSO	dimethylformamide
DMF	dimethyl sulfoxide
PCE	power conversion efficiencies
BHJ	bulk heterojunction
D/A	donor/acceptor
ODCB	1,2-dichlorobenzene
MS	mass spectrometry
MP	melting point
EA	elemental analysis
NFA	non-fullerene acceptor
RT	room temperature
DBCA	dibromoisocyanuric acid
TBCA	tribromoisocyanuric acid
DBDMH	dibromodimethylhydantoin

1. INTRODUCTION

1.1. Context

It is generally recognised that the global increase in population and an accompanying rapid change to ever more energy intense lifestyles is having a detrimental effect on our planet. Since the industrial revolution, our way of consuming has changed in such a pace we now need to face the consequences. Indeed, in just a couple of centuries, humans have developed knowledge and tools that could not even have been dreamed of in the preceding thousand years. It is interesting to remember that we now live in a society where new generations of smartphones are launched every year, while our oldest ancestors kept using the same flint tools for generations and generations (Figure 1).[2]
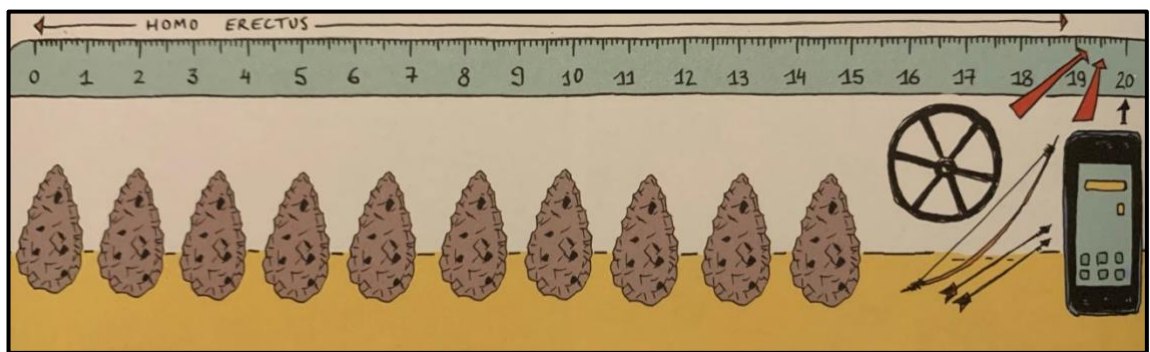
Figure 1. *Drawing showing on a time scale how fast everyday tools have changed in the last centuries (taken from[2]).*

Because of this race towards progress, the world is now engaged in what looks like an unstoppable process of mass production. The unintended upshot of this is the generation of ever-increasing quantities of waste material, be those physical products such as packaging or CO_2 which causes climate change. As the scale of this problem becomes clear, politicians, industrialists, and the general population are progressively changing their ways of life and thinking. This has resulted in the development of new solutions from all corners of the world, and for all sectors.

The chemical and pharmaceutical industries have long been known to be significant sources of pollution, and therefore have a vital role to play by reducing their environmental impact. Fortunately, they are currently investigating new technologies and processes which are less environmentally

costly. To achieve this, more money has been invested over the last few years for scientists to investigate new concepts to mitigate environmental impact which have collectively become known at *green chemistry*. According to the American Chemistry Society (ACS), "sustainable and green chemistry […] is just a different way of thinking about how chemistry and chemical engineering can be done." With that idea in mind, twelve principles have been proposed that can be used when thinking about the design, development and implementation of chemical products and processes (Figure 2).
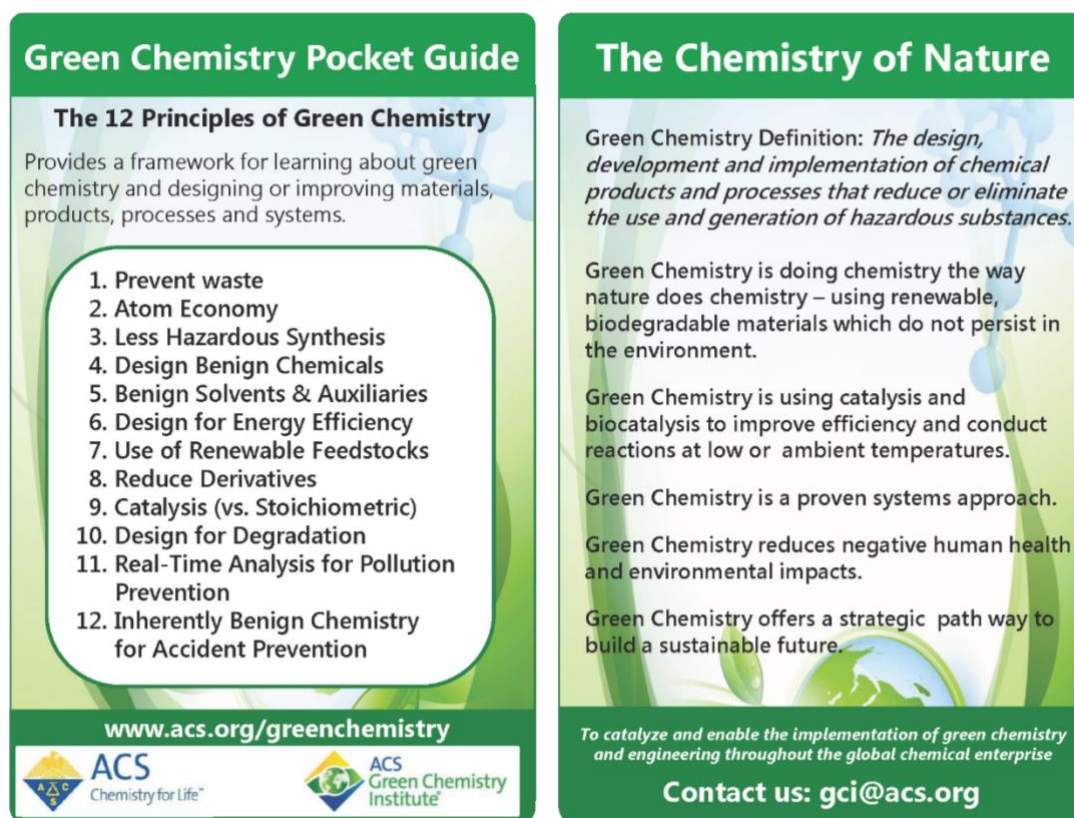
Figure 2. *The ACS Green Chemistry Pocket Guide on the 12 principles of green chemistry (taken from[3]).*

These principles enable scientists and engineers to protect and benefit the economy, the people, and the planet by finding creative and innovative ways to reduce waste, conserve energy, and discover replacements for hazardous substances. The envisaged innovations cover all the technologies that already exist and many others which are, hopefully, still to be invented. Among them can be found continuous flow reactors,[4,5] lab microwaves,[6–8] UV lamps[5] for reaction initiation and, most importantly for this report: mechanochemistry.

The next section will then define and discuss the history of this technique, how it works, its pros and cons, and why the science community is getting so excited about it.
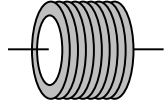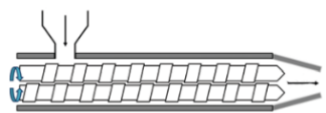
1.2. Mechanochemistry

According to IUPAC, a mechano-chemical reaction is defined as "a chemical reaction that is induced by the direct absorption of mechanical energy". The first mechanochemical reactions were performed by grinding chemicals together with a mortar and pestle (Table 1), sometimes referred to as "grindstone chemistry". This technique has the advantage to be solvent-less and only dependent of the physical strength of the operator. However, for the same reason, it has the limitations of not being practical unless reaction times are very short, and it is not generally accepted as a routine technique to do chemistry.

To overcome these deficiencies, automated devices called *ball mills* have developed which enable good reproducibility while still being more eco-friendly by using less energy and producing less waste than in conventional solvent-based batch-type reactions.

Originally, ball mills were designed to grind soils or rocks, to get fine powders of minerals such as sand. It was only in the early 1990's,[9] that chemists started to investigate their efficiency to perform chemical reactions. Indeed, the application of mechanical forces through the use of ball mills offers many advantages over traditional solvent-based strategies.[10–15] Obviously, the most significant advantage is to that reactions are carried out under solvent-free or solvent-less condition.[i12,13] Additionally, however as the reagents are not dissolved, they are at maximum concentration, which can result in a significant decrease of the reaction time. All of this leads to experiments which are very easy to run, manage and treat, while being more environmentally friendly compared to solvent-based reactions.

Table 1. *Comparison of five different techniques to do chemistry.*

	Reproducibility	Sustainability	Scale-up capability
Mortar and pestle	✘	✔	✘
Solvent-based	✔	✘	✘
VBM (MM)	✔	✔	✘
Flow reactor	✔	✔ but solvent-based	✔
Twin-screw extruder (TSE)	Yet to be proved	✔	✔

In addition to the advantageous green credentials of mechanochemistry, it has been shown that this technique can also alter chemical reactivity and selectivity compared to the analogous solution-based protocols.[15] As a consequence, solvent-free milling can lead to different product compositions or equilibration mixtures than in solution (Schemes 1 and 2).
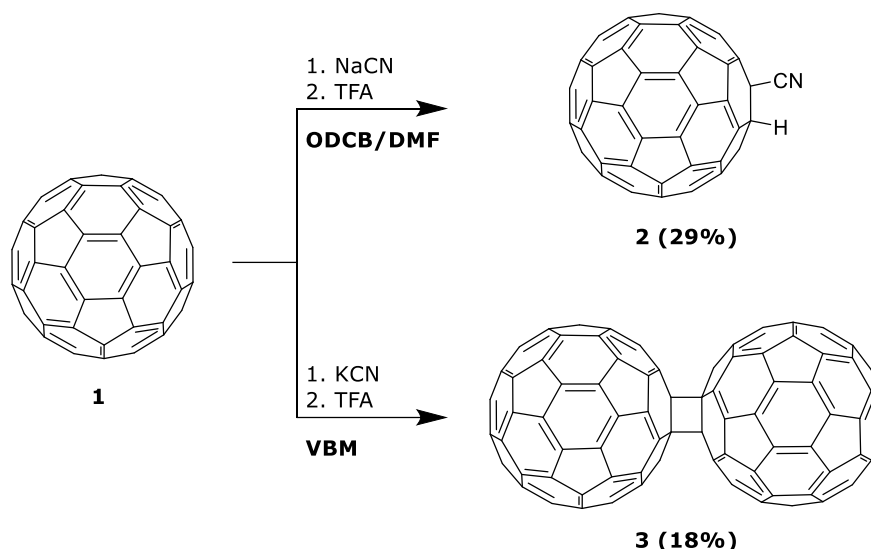
Scheme 1. *Difference in chemical reactivity of C_{60} in solution and solid-state conditions.*[15]

solution-phase MeCN	neat or liquid-assisted grinding (MeCN)
mixture composition	mixture composition
4 : 25%	4 :
5 : 25%	5 : } 2%
6 : 50%	6 : 98%
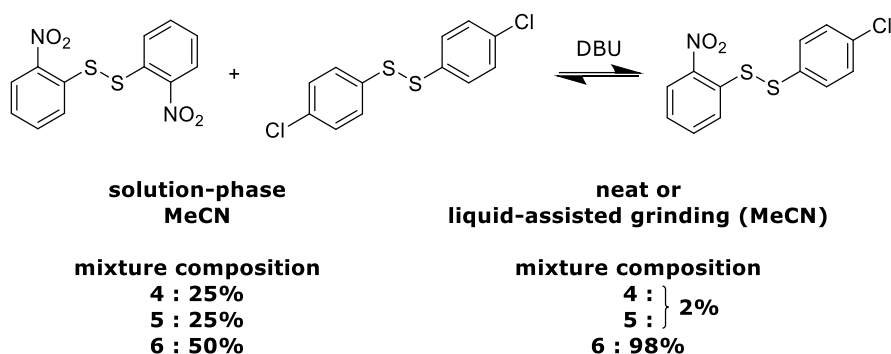
Scheme 2. *Difference in the equilibration composition of a disulphide metathesis reaction in solution and solid-state conditions.*[15]

Some research groups have even seen another fascinating potential for mechanochemistry: the ability to reproduce or simulate what happened at the surface of the very early Earth, and try to predict prebiotic scenarios for the synthesis of α-amino acid derivatives (Scheme 3).[16] This area of science, connecting chemistry (astrochemistry) and biology (exobiology), is already studied in several universities,[17] but only investigated very recently in the solid-state, using ball mills.

CN^- source: NH_2COH, $[Fe^{2+}(CN)_6]$, $[Fe^{3+}(CN)_6]$, $Fe^{3+}[Fe^{2+}(CN)_6]$
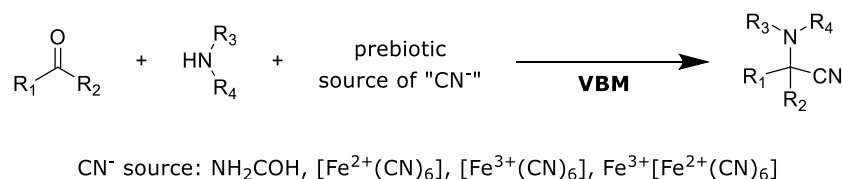
Scheme 3. *Mechanochemical α-aminonitrile formation with prebiotic sources of cyanide.*[16]

There are two types of commercial ball mill designed for routine use in research laboratories. The simplest is the vibratory ball mill (VBM, Figure 3) which is suitable for small laboratory scale chemistry (few milligrams to hundreds of milligrams). It oscillates a horizontal milling plane at high frequency and must carry two identical reactors with similar reagent loadings to keep a perfect balance. These reactors, as well as the balls used as grinding media, can be made of different type of material, depending on the nature of the chemicals used (acidity, inorganic materials, etc). It has been proposed by the James group[18–20] that their composition, among other parameters, can also lead to different type of reagent fragmentation which are described, from the softer stress to the stronger, as: abrasion, cleavage, and fracture.

The next larger scale of lab-scale grinding equipment is the planetary ball mill (PBM, Figure 3). PBMs are suitable for small to medium laboratory scale chemistry (up to 100s of grams). This instrument operates by imitating the rotation of the planets around the Sun in the solar system. The grinding jars in PBMs can be filled with significant numbers of milling balls, in order to scale up reaction quantities or reach higher temperatures.[21,22]
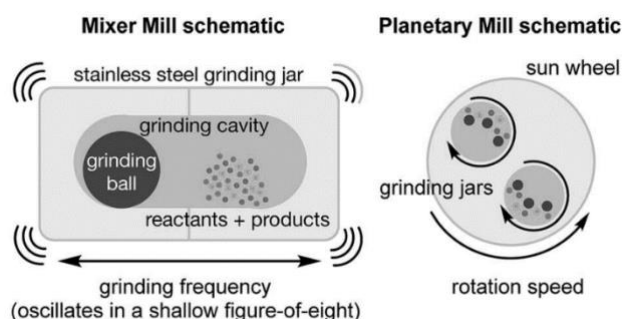
Figure 3. *Working principle of the vibratory ball mill (VBM, left) and the planetary ball mill (PBM, right) (taken from[23]).*

An important factor concerning both VBMs and PBMs is the type of grinding media used in these reactors. The volume, composition, mass, density of the balls, have a significant influence in the process. The quantity of these balls is also an important variable because it changes the free volume in the reactor, and thus the type of fragmentation (Table 2). This is directly linked to another parameter called *milling load*[ii]. This parameter important because the more filled a jar is with starting materials, the less thermal energy is created due to damping of the impacts between the milling balls and the inner walls of the jar.

Table 2. *Comparison of the free volume (%) in a 25 ml grinding jar, depending on the number and diameter of milling balls filled in (sample volume not included).*

Number of balls	Ball diameter		
	∅ 10 mm	∅ 12 mm	∅ 15 mm
1	98%	96%	**93%***
2	96%	**93%***	**86%***
3	94%	**89%***	79%
4	92%	**86%***	72%
5	**90%***	82%	65%

* Recommended ball charge by manufacturer. Recommended sample amount is 4-10 ml for a 25 ml grinding jar.

The third type of device is not originally designed for chemistry but can adapted to carry out mechanochemistry on an industrial scale is the twin-screw extruder. In 2019, during the IUPAC World Chemistry Congress that celebrated the 100th anniversary of the union (and incidentally, the 230th anniversary of the original publication of Antoine Lavoisier's "Traité Élementaire de Chimie", considered by many to be the first modern chemistry textbook), a comment piece entitled "top ten emerging technologies in chemistry" was released. Among these ten technologies were featured two green chemistry technologies: flow chemistry and chemical extrusion.[24] The latter is still barely known in the chemistry community but promised to a bright future for the industry. Indeed, it allows to perform solvent-less milling in a continuous way.

The working principle of an extruder (Figure 4) is very simple and similar to the one of flow chemistry in solvent-based systems. The solid reactants are added in the grinding chamber through the feeder (several feeders can be set up to add reactants in different timings). The starting materials are mixed enabling the reaction to occur and resulting product emerges from the nozzle. As is the case for reactions carried out in a ball mill, a small amount of liquid can be added in the system which can aid the synthesis. Some extruder models also have grinding areas that can be heated, if necessary.

This equipment can be heavy and bulky and has yet to be seen widely in research laboratories. Therefore, why the number of publications related to reactive extrusion is still very limited, and the concept reliability yet to be proved. However, partnerships with industries possessing that kind of equipment have resulted in several proof of principle studies. For example, Frédéric Lamaty's group in France, demonstrated peptide couplings[25] (Figure

4, left), while Sabyasachi Gaan's group in Switzerland, illustrated a Michael addition[26] (Figure 4, right), both in reactive extrusion. It can also be used for pharmaceutical formulation, according to Ali Nokhodchi's work with hot melt extrusion.[27–30] More recently, the group of Stuart L. James has described continuous, solvent-free synthesis of commodity perylene diimides.[31]
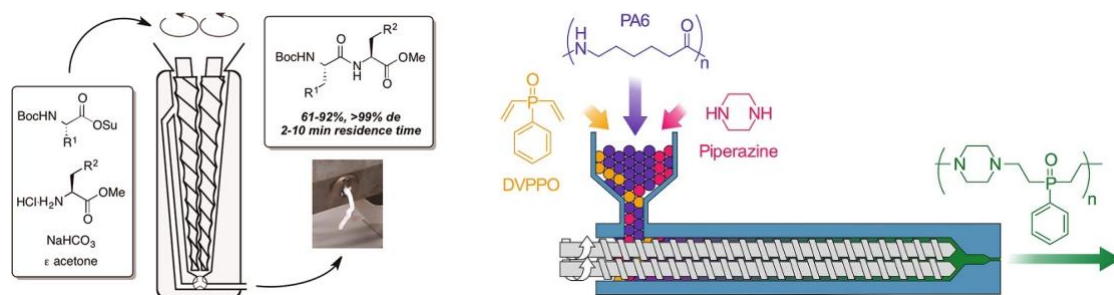
Figure 4. *Peptide couplings (left) and Michael addition (right) in a twin-screw extruder.*[25,26]

Nowadays, not only mechanochemistry but all sustainable synthesis techniques are getting more and more popular and considered as reliable processes, which contrasts with the scepticism with which they were viewed in the previous decades.

This section has introduced the concept of mechanochemistry and the highlighted its merits compared to solution state chemistry. It is now important to consider target molecules that would benefit from synthesis by these new techniques. Molecules used in organic electronics, for example those based on diimide containing motifs, have received little attention in mechanochemical synthesis. In addition, they frequently require harsh conditions and solvents to be synthesised. Therefore, the next section will introduce the concept of organic photovoltaics and discuss the synthetic methods used to produce them these molecules and polymers.

1.3. Organic photovoltaics

It is widely agreed that renewable energies, and more specifically, solar energy, will play a key role in solving serious environmental problems and the terawatt energy challenge the world is facing. To overcome these problems, a particularly promising and active area of research is the field of photovoltaics, and especially organic photovoltaics (OPVs), also known as organic solar cells (OSCs).

The photovoltaic effect was experimentally demonstrated first by French physicist Edmond Becquerel in 1839. Becquerel demonstrated that absorption of light by specific materials creates electrical voltage. This process was studied intensively in the 1950s resulting in the first silicon solar cells produced commercially. This was achieved using results stemming from the work of three physicists at Bell Laboratories[32] that created the first practical solar cell showing a power conversion efficiency (PCE) of 6%. This parameter is defined by the fraction of incident power converted into electricity. Because of the prohibitive costs of silicon solar cells at that time, their manufacturing is limited for the use in specific programs such as space exploration. The first solar-powered satellite, Vanguard 1 (Figure 5), has travelled more than 197,000 revolutions around the Earth in the 50 years it has been in orbit, and still counting. This application paved the way for more research to decrease costs and increase production.

In the 1980's, the first solar parks[33] were created in California, by the Atlantic Richfield Company (ARCO) solar-based unit, which is now part of the BP group. Finally, in the 2000's, as technology costs have decreased and the efficiency of solar cells has increased, residential solar power has become more popular and accessible in any home.
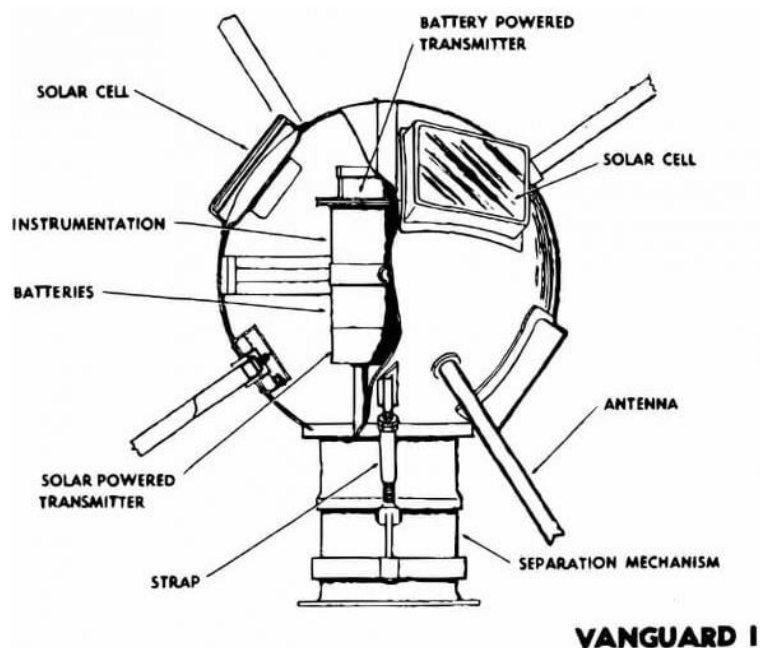
Figure 5. *World's first solar-powered satellite Vanguard 1 (taken from[34]).*

Today, solar cells can be classified into three generations. First one cells are the conventional, traditional, or wafer-based cells, made of crystalline silicon such as polysilicon and monocrystalline silicon. Second generation cells are called thin film solar cells and made of an active material between two panes of glass. This material can be a thin film of amorphous silicon, cadmium telluride (CdTe), copper indium gallium selenide (CIGS) or gallium arsenide (GaAs). When multiple thin films are used in one single device, they are termed multijunction cells. As access to those rare metals is getting more costly because of inflation and resource depletion, a third generation of solar cells emerged. These PVCs include several thin-film technologies which are also sometimes described as emerging photovoltaics.

The most developed of these next generation PVCs are dye-sensitised solar cells, perovskite solar cells, quantum dot solar cells[35] and organic solar cells (OPVs). In less than a decade, the increasing interest for emerging photovoltaics already resulted in the creation of OPVs that can reach PCEs (up to 18%[36]) almost matching the best traditional crystalline silicon photovoltaics (PCE = average of 20 to 27%). Even though OSCs do not exhibit as good PCEs as multijunction cells (up to 47.1%[37]), they remain very interesting because the compounds used are inexpensive to synthesise and no precious metals are necessary. A lot of research has been invested into these technologies as they promise to achieve the goal of producing low-cost, high-efficiency solar cells.

Figure 6 shows the structure and composition of an OPV and how it converts solar energy into electricity (Figure 8). An OPV can be described as a device that is made of a photo-active layer sandwiched between two interfacial layers and electrodes (most frequently indium tin oxide alloy as the anode, and aluminium or calcium as the cathode). The structure of this photo-active layer can vary, depending on the type of compounds that compose it. It contains electron donor and acceptor molecules or polymers that together form a bilayer (Figure 6, left), or more frequently, a bulk heterojunction (BHJ) structure (Figure 6, middle and right).
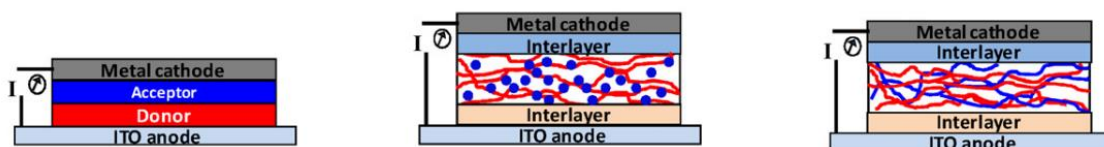
Figure 6. *Representative composition of different types of photo-active layer in OPVs (taken from[38]). Left: a single heterojunction. Middle: a polymer-donor and molecular acceptor BHJ. Right: "all-polymer" BHJ.*

Figure 7 shows schematically the working principle of electricity generation in OPVs. Briefly, when a photon is absorbed in an electron donor region of the BHJ, an electron is promoted to an excited energy level, leaving a positive 'hole' behind. This excited electron and hole pair is termed an exciton. Subsequently, the exciton diffuses to the donor/acceptor (D/A) interface, where it dissociates by electron transfer to generate free charge carriers (a hole and an electron). Lastly, these free charge carriers are separated and transported to the electrodes, where they are extracted.
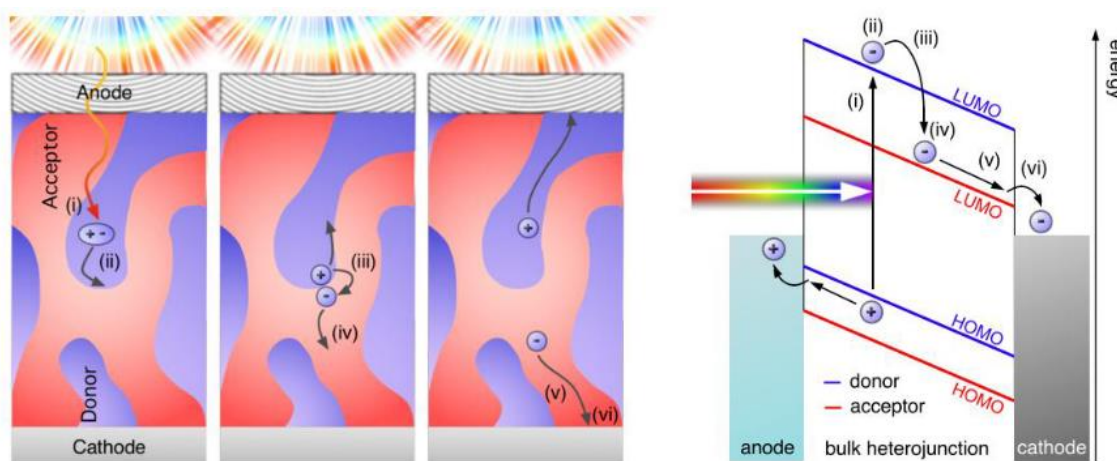
Figure 7. *Introduction to OPVs (taken from[35]). Left: cross-section of the conceptual device structure of OPVs (BHJ active layer in the middle). Right: the operating mechanism of OPVs. (i) absorption of photons and creation of excitons; (ii) diffusion of excitons to D/A interfaces; (iii) dissociation of excitons to free charge carriers at D/A interfaces; (iv) separation of the free charge carriers; (v) charge transport to the electrodes; (vi) charge extraction.*

Processing of the materials to optimise the morphology of the layers within OPVs can have a dramatic impact on the efficiency of the system. However, optimising electronics of the chemical constituents of the OPV is still a major field of discovery.

There are many examples of organic electron donor molecules and polymers reported in the literature, forming a large database available for researchers and industrials. The most successful example concerns conjugated polymers based on cyanated poly(phenylenevinylene) backbones, also commonly

called poly(phenylene vinylene)s (*PPVs)* (Figure 8). These were the first electron donors investigated independently by the groups of Friend[39] and Heeger[40]. Using the bulk heterojunction approach, both teams demonstrated that photogenerated excitons in the polymer layer can be efficiently dissociated into free carriers at the photoactive blend interface. Therefore, many variants of this class of donor polymer have been designed, such as poly[2-methoxy-5-(2'-ethylhexyloxy)-1,4-phenylene vinylene] (Figure 8, MEH-PPV, left), or poly[2,5-dimethoxy-1,4-phenylene-1,2-ethenylene-2-methoxy-5-(2-ethylhexyloxy)−(1,4-phenylene-1,2-ethenylene)]) (Figure 7, M3EH-PPV, right).

MEH-PPV   **M3EH-PPV**
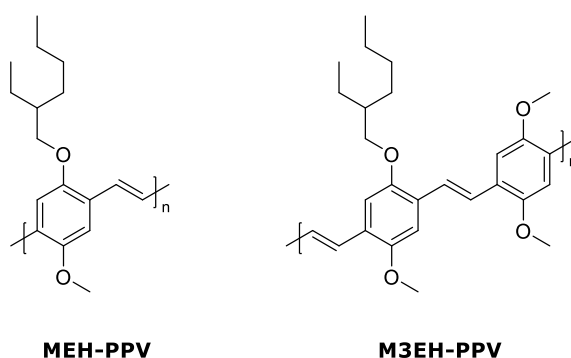
Figure 8. Two examples of PPV electron donor polymers.

In contrast the electron acceptor component of OPVs is a less mature field. This section introduces some of the most influential examples published in the literature. As noted above, the first, widely studies small molecule demonstrated to behave as an electron acceptor in OPVs were the fullerenes. This family of non-planar carbon compounds, popular for their football ball-like shape, were characterised for the first time at the University of Sussex.

The initial discovery began in the 1970s with Sir Harry W. Kroto FRS and Doctor David Walton investigations of unsaturated carbon configurations. They developed methods for synthesising long chain polyynes and polyynylcyanides such as HC_5N, HC_7N and HC_9N which had been detected in the cloud material of the interstellar medium, and whose vibration-rotation dynamics had been studied by microwave spectroscopy. Concurrently, at Rice University, Texas, the group of Professor Richard E. Smalley and Professor Robert F. Curl, Jr. was developing a technique where they used laser vaporisation of a suitable target to produce clusters of atoms. This work lead

Kroto to apply this experimental technique to graphite targets, in the hope that the apparatus would be ideal to probe the formation of carbon chains.

The resulting experiment probed the carbon plasma produced by time-of-flight (TOF) mass spectrometry laser vaporisation. This resulted in the presence of peaks corresponding to large carbon chains/clusters, including the yet unidentified but very stable C_{60} and C_{70} molecules as evidenced by intense signals at m/z = 720 and 840 in the mass spectrum. This suggested carbon molecules with sixty and seventy carbon atoms respectively were forming.[41] The research group concluded after several reactivity experiments, that the most likely structures were spheroidal molecules. They were named after Mr Richard Buckminster Fuller because of the architecture of his geodesic dome structures, which contained pentagons as well as hexagons (Figure 9) ultimately leading to the groups receiving the Nobel Prize for Chemistry in 1996.
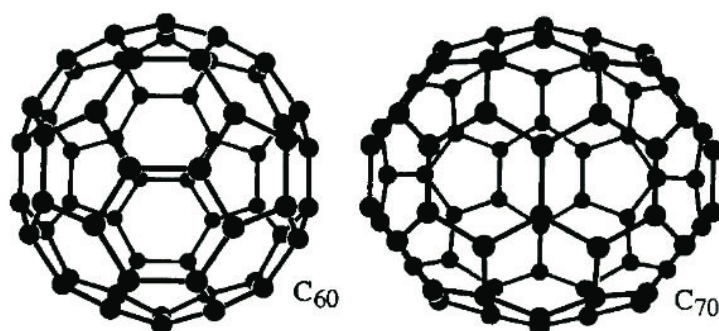
Figure 9. *Buckminsterfullerenes: C_{60} (left) and C_{70} (right).*

Subsequently, functionalised fullerenes have been the most studied and used as electron acceptors for OPVs are called $PC_{61}BM$[42] and $PC_{71}BM$[43] (for phenyl-$C_{61/71}$-butyric acid methyl ester). These can be readily synthesised using freshly prepared methyl 4-benzoylbutyrate *p*-tosylhydrazone under nitrogen atmosphere (Scheme 4).[42] Those bulky molecules could be used in association with molecular donor compounds (Figure 6, left). Mostly, however, they are used with polymer-donor compounds (Figure 6, middle), such as PPV polymers (Figure 8), as they self-assemble into a favourable BHJ morphology. Fullerenes have been considered for a long time as the best electron acceptors because of their high electron mobilities, and their ability to form interpenetrating networks with donors, which is favourable for charge

separation and charge transport. Under the most favourable conditions, the highest PCEs recorded for those devices were as high as 11%.[44–51]
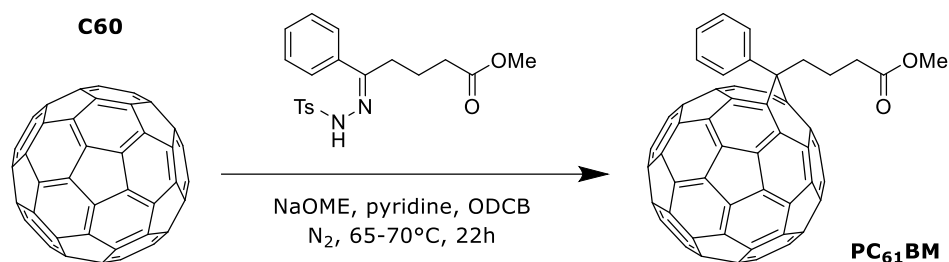
Scheme 4. *Synthesis of PC$_{61}$BM. ODCB = 1,2-dichlorobenzene; Ts = tosyl.*

However, despite these promising characteristics, fullerene-based OPVs exhibited serious drawbacks, including poor light-absorption properties,[52] limited energy-level tunability,[53] low access to functionalisation due to the fullerene structure, high synthesis costs, and morphological and/or photochemical instability.[54] Because of that, chemists started to focus on the synthesis of non-fullerene acceptors (NFAs), and most importantly, polymer-based acceptors. These offer potential advantages, including long-term mechanical and thermal stability, but above everything else, a superior control of solution viscosity, a crucial factor for the solution processing of large-scale OPVs.[38,55]

Although the first bilayer OSC using a NFA (made of copper phthalocyanine and PDI derivative) was reported in 1986 exhibiting a modest PCE of 1%[56], researchers took some time to develop all-polymer-based OPVs (Figure 6, right) that would compete with known fullerene-based OPV. It is only from 2015 that concerted materials synthesis and device optimization efforts have increased PCEs for NFA OSCs from 6% to >13% thus exceeding fullerene analogues.

Today, NFAs can be classified into two main categories: rylene diimides and fused-ring electron acceptors (Figures 10 and 11). From the 76 compounds that have been exhaustively reviewed in 2018 by Zhan's group,[57] some of them have been picked as examples for this report. Several classes of compounds make up the family of rylene diimides: perylene diimide (PDI) and naphthalene diimide (NDI) polymers, or PDI small molecules. PDI copolymers have been reported with different functional groups such as carbazoles (Figure 10, top), dithienothiophenes, thiophenes, or simply

vinylenes, as well as NDI polymers with different possible combinations of thiophene- (Figure 10, top) or selenophene-based groups. OSCs based on such NDI polymer acceptors still exhibit the highest known PCE values for all-polymer solar cells. Regarding small molecule acceptors, two or more PDI molecules can be linked directly together (Figure 10, bottom), or constrained with the introduction of a conjugated planar or non-planar bridging group.

PDI-carbazole   **NDI-bithiophene**
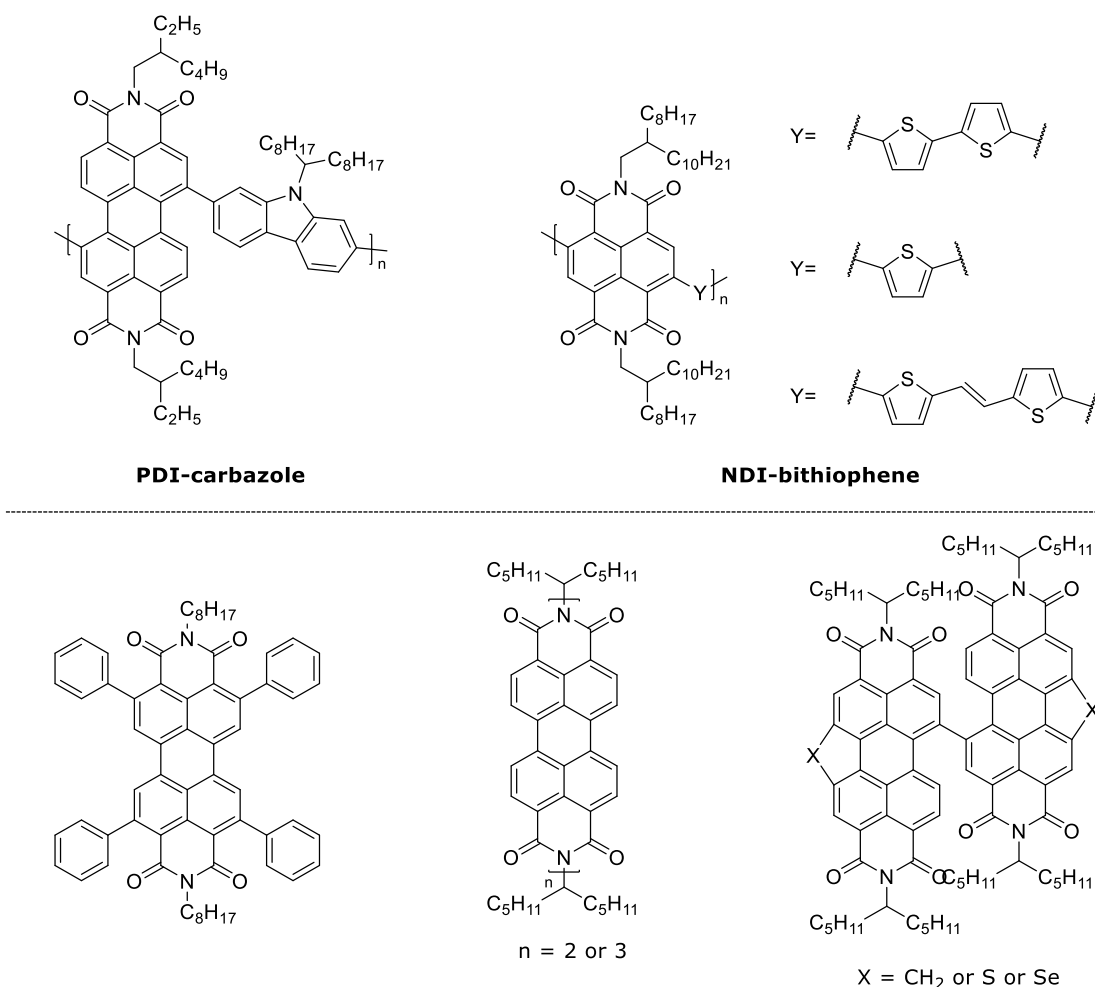
Figure 10. *Examples of rylene diimides electron acceptors.*
Top: PDI- and NDI-based polymers. Bottom: PDI-based small molecules.

The most significant alternative to the PDI/NDI materials discussed above are those based on fused-ring acceptors. These consist of two strongly π-electron-withdrawing termini linked by a planar π bridge containing fused rings that are substituted with aryl or alkyl side chains that project above or below the plane.[58] This class of compounds is the closest to fullerene-based acceptors in term of electron affinities and long-wavelength absorptions. Modifications of the fused-ring core and electron-withdrawing groups can be used to tune many parameters such as the absorption wavelength, ionization

energy and electron affinity. Indacenodithiophene derivatives (Figure 11, left), for example, are among the most frequently used cores, while benzothiadiazole-rhodanine derivatives (Figure 11, right) are typical end groups of choice.
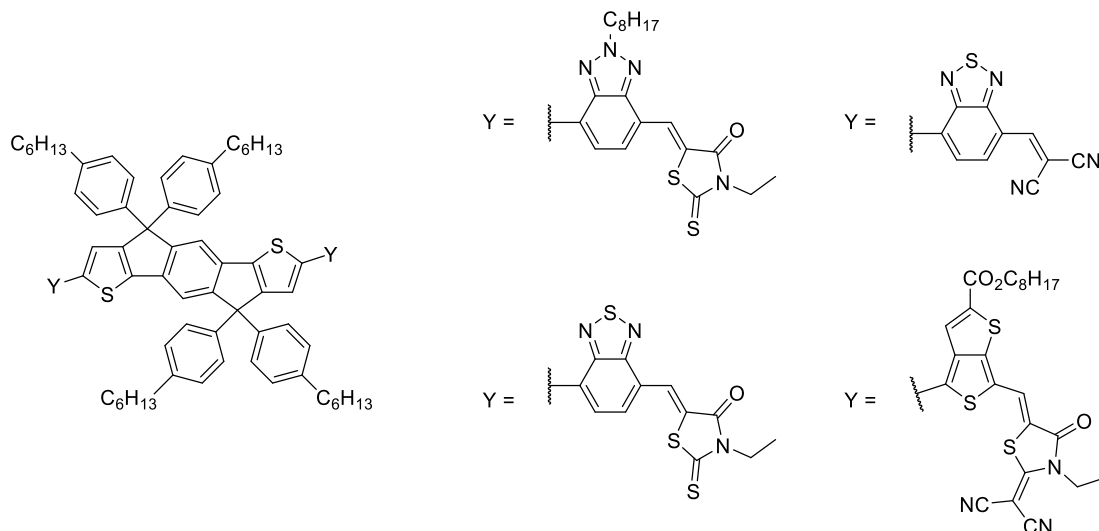
Figure 11. *Examples of fused-ring electron acceptors.*

At the time of writing of this report, the research group that showed polymer-based OPVs with the best performances (PCE of more than 17%[59]) is the one of Professor Alex K.-Y. Jen from the City University of Hong Kong. To help researchers, an online database[60] exists with all the polymers and oligomers identified as donor or acceptor material for OPV application, which allows researchers to compare and design new devices using data from the broad range of OPVs that have been developed up to now.

Considering all the examples presented in this section, the compounds chosen to be synthesised are NDI-based acceptors (Figure 10, top). This is because of their strong light absorption, stability, planarity, and their ease of characterisation by ^{1}H NMR spectroscopy. In addition, unlike fullerenes, NDIs can be readily used as monomers to produce polymers suitable for use as electron acceptor materials in OPV applications. After extensive bibliography research, and as far as we know, no publication reported the synthesis of such compounds by mechanochemistry yet. These are valuable and important materials that currently cannot be made in a solvent-free way. Therefore, achieving this for the first time could have a real impact on society.

1.4. The solid-state synthesis strategy inspired by the solvent-based conditions reported in the literature

The aim of this project is to open the way towards sustainable and clean manufacturing of the next generation of organic photovoltaics for industry. Here, the idea is to try to design novel pathways for the synthesis of NDI-based electron acceptor polymers using an eco-friendly technique: mechanochemistry.
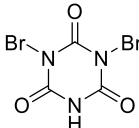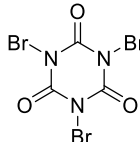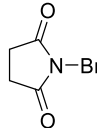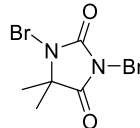
One typical example of synthetic methodology to produce those kinds of compounds would be the one presented in Scheme 5, using naphthalene-2,3-dicarboxaldehyde (NDA), an inexpensive reagent, as starting material.
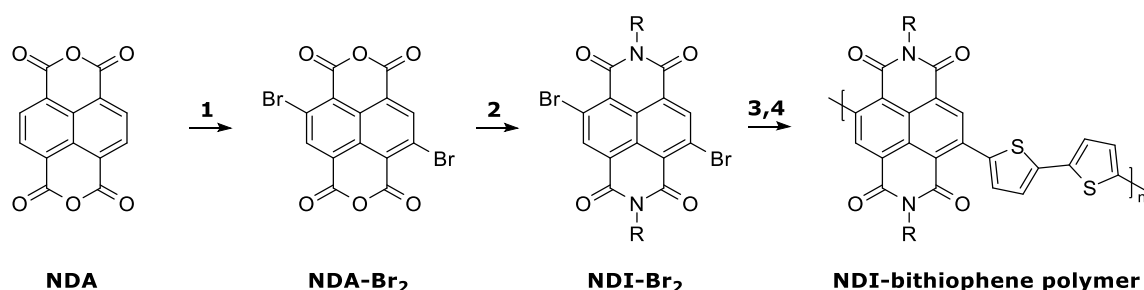
Scheme 5. *Generic scheme of the synthesis of an NDI-based polymer from NDA.*

Some publications have reported high conversion of NDA to NDA-Br$_2$ in solution, using an organic brominating agent and a strong acid (Table 3).

Table 3. *Solvent-based NDA bromination bibliography.*

brominating agents : **DBCA**   **TBCA**   **NBS**   **DBDMH**   **XBr**

Entry	Brom. agent	Conditions (†)	% Yields (‡)	Refs
1	DBCA	H$_2$SO$_4$/Δ (12-20)	33-100 (83)	61–65
2	DBCA	H$_2$SO$_4$/RT (5-12)	76-82 (80)	66–68
3	DBCA	oleum/RT (7)	40-83 (67)	69–71
4	DBCA	oleum/Δ (48)	82	72
5	DBCA	H$_2$SO$_4$/SO$_3$/Δ (43)	82	73
6	DBCA	H$_2$SO$_4$/SO$_3$/RT (5)	75	74
7	DBCA	H$_2$O/RT (7)	82	75
8	DBDMH	H$_2$SO$_4$/RT (10-48)	89-95 (92)	66,68
9	DBDMH	H$_2$SO$_4$/Δ (48)	46	76
10	TBCA	H$_2$SO$_4$/RT (12)	76	77
11	NaBr	H$_2$SO$_4$/SO$_3$/Δ (16)	85	78

† Reaction time window in hour(s).
‡ Average yield.

In our hands, we tried to reproduce these reactions, it indeed showed consumption of the NDA starting material but the desired dibrominated NDA-Br$_2$ (Scheme 5, step 1) was complex to isolate in high purity. This is likely to be because of selectivity issues during bromination and, like many other large polyaromatic hydrocarbons, poor solubility. In fact, their isolation is hindered by the production of a statistical mixture of mono-, di-, tri- and tetra-brominated NDI residues (Scheme 6), as described in a few publications.[79–81]
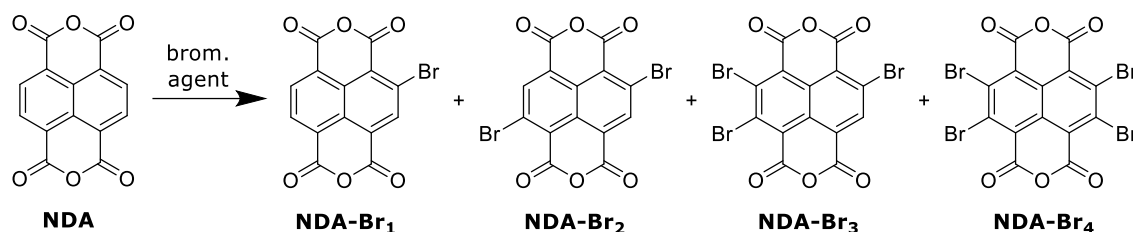
Scheme 6. *NDA bromination resulting in a mixture of n-brominated-NDI residues.*

Furthermore, their preparation in solution often requires long reaction times at high temperatures, and with large amounts of harmful solvents such as DMF, or concentrated acids. With this in mind, we sort to optimise the mechanochemical synthesis of NDA-Br$_2$ using a range of brominating agents in different conditions.

Regarding the synthesis of NDIs by imidisation (Scheme 5, step 2), many examples in the literature report that the reaction is relatively straightforward in solvent-based conditions, and the yields usually over 80% when NDA is used as starting material. However, as soon as NDA is replaced by dibrominated NDA-Br$_2$ as starting material, yields tend to drop and rarely exceed 50%, as can be seen with the examples presented in the table (Table 4).

Table 4. *Solvent-based dibrominated NDA imidisation bibliography.*
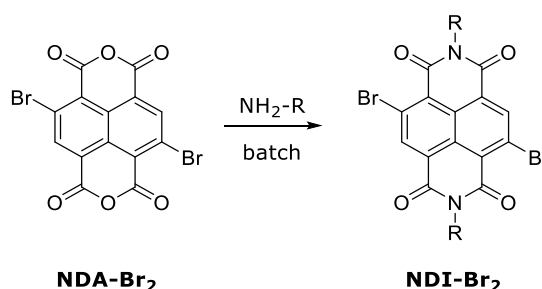
Entry	NH$_2$-R group	Conditions (†)	% Yields (‡)	Refs
1	ethylhexylamine	AcOH/Δ (1.5-21)	10-55 (35)	[61,63,69,82–87]

Entry	NH$_2$-R group	Conditions (†)	% Yields (‡)	Refs
2	octylamine	AcOH/Δ (1-24)	22-88 (42)	65,74,87–90
3	hexylamine	AcOH/Δ (1.5-4)	16-35 (27)	87,91,92
4	ammoniac	ammonium acetate/AcOH/Δ (1-6)	40-84 (67)	63,91,93

† Reaction time window in hour(s).

‡ Average yield.

Both situations (Steps 1 and 2, scheme 5) will be experimented in the ball mill, using several aromatic and non-aromatic amines in different conditions to see how the reaction behave in the solid state.

Finally, the last steps (Scheme 5, step 3 and 4) are briefly introduced at the end of the results and discussions section. Step 3 consists of the substitution of the two bromines by bithiophene groups, while step 4 is a polymerisation. Several pathways exist, especially for step 3 and the synthesis of the bithiophene-NDI monomer. As far as we know, only three publications have successfully reported the synthesis of such NDI monomers in solvent-based conditions. Both of them describe palladium(II)-catalysed Stille coupling reactions to afford the desired product (yield 72%[94] and 86%[95]), while the third one describes a palladium(II)-catalysed C-H activation reaction (yield 40%[96]). In the meantime, solid-state Suzuki-Miyaura cross-coupling reactions have also been successfully reported in the literature,[97] using NDI-like olefin-accelerated additives. This leaves us several promising opportunities to experiment in order to reproduce the synthesis of the bithiophene-NDI monomer by mechanochemistry.

In brief, the following results and discussions section presents the strategies used to synthesise and characterise all the products that could be isolated in solvent-based and mechanochemical processes. In the latter case, such reactions have not been investigated for this class of compounds before. Finally, a brief list of future avenues for research that could not be attempted in the time available will be identified at the end of this report.

2. RESULTS AND DISCUSSIONS

2.1. Mechanochemical synthesis of NDI derivatives

This section is divided in three subsections discussing the different routes investigated to synthesis brominated NDI derivatives as outlined in Scheme 7. It can be seen that it would be possible to brominate the naphthalene-2,3-dicarboxaldehyde (NDA) then carry out the imidisation, which is the only methodology described in the literature (Scheme 7, routes i. then ii.). Also, it was thought that it could be interesting to study the reversed synthetic pathway by first, performing the imidisation of NDA then the bromination (Scheme 7, routes iii. then iv.). In that regard, the imidisation step of NDA will be the first one presented in the next subsection.
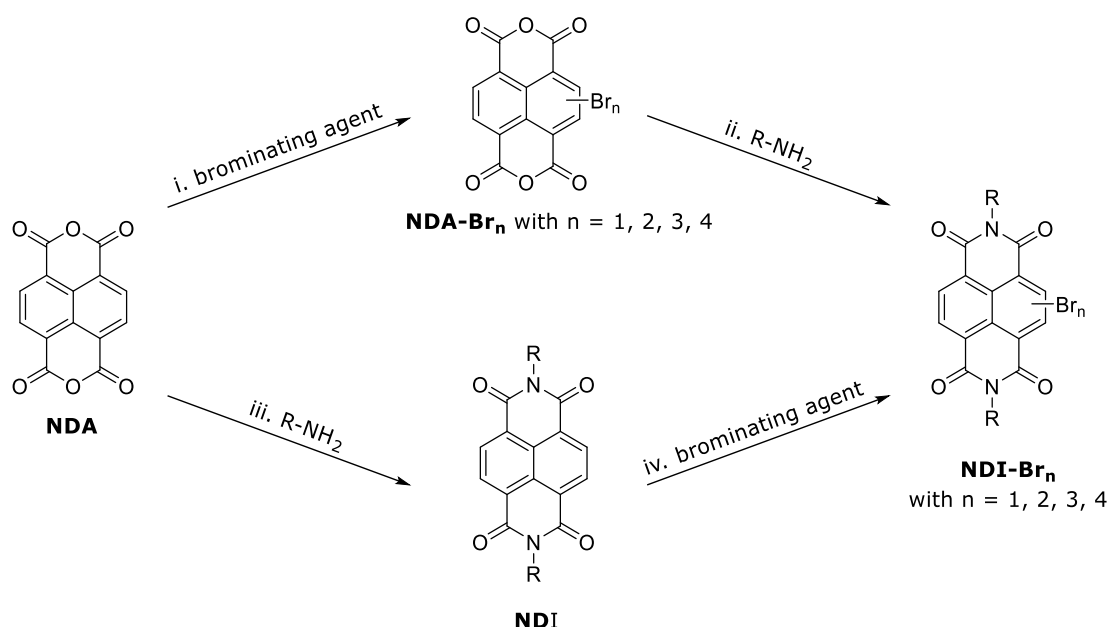
Scheme 7. *Overall scheme of the two different synthetic routes to brominated NDIs.*

2.1.1.   Synthetic investigations into NDA imidisation

As indicated in the introduction, the imidisation of NDA is the most widely studied reaction in solvent-based conditions. Therefore, the investigation of this reaction in the solid-state was selected as the initial target for optimisation using mechanochemistry. The first reactions were conducted using 2 equivalents of 2-ethylhexylamine, neat in a 10 mL stainless steel grinding jar, and 30 minutes milling time at 30 Hz. The spectra obtained by ^{1}H NMR spectroscopy (Figure 12, top spectra) showed several aromatic

environments, while only one was expected in the structure of the targeted NDI product. Therefore, it was proposed that the reaction had not gone to completion and that the colourless product isolated was the chemical intermediate *iNDI* with opened rings (Figure 12, top left structure). Indeed, this intermediate has two amide protons and two carboxylic acid protons, allowing two different isomers and more hydrogen couplings concerning the aromatic protons (Figure 12, top spectra, blue/red/green boxes).

To try to push the reaction towards completion and, following the literature concerning solution state synthesis,[98] it was decided to work under moisture free conditions by flushing argon in the jar, to avoid any hydrolysis side-reaction. This did not afford any better result, so the temperature parameter was more carefully considered to drive the ring closing which requires loss of water. Indeed, a ^{1}H NMR spectroscopy analysis of the iNDI product after heating in DMSO at 130°C for a few minutes resulted in the simplification of the NMR spectrum which now exhibited a single peak at 8.76 ppm, consistent with the proposed structure (Figure 12, bottom molecule). It was concluded that the ring closing had occurred, and that the temperature was a crucial parameter for the cyclization of iNDI.
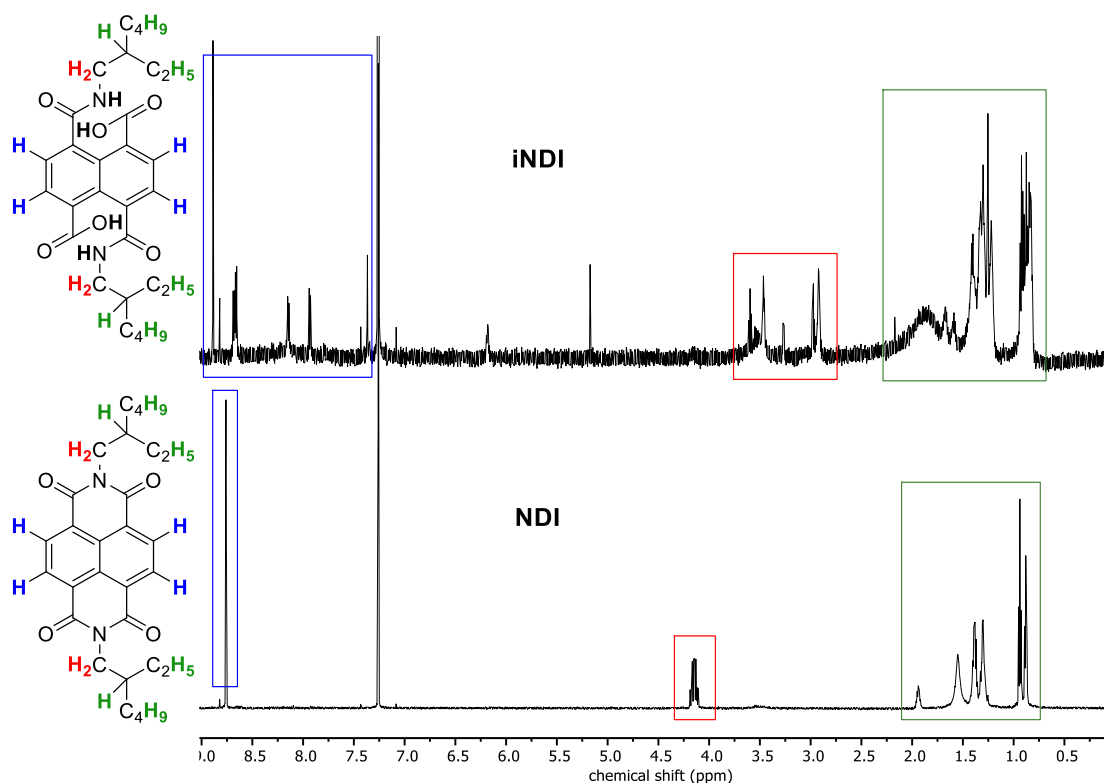
Figure 12. *^{1}H NMR spectra of iNDI and NDI, showing the importance of the temperature for completion of this reaction. Boxes colour matches with protons colour from the structures.*

Blue boxes: aromatic protons. Red boxes: protons from the closest -CH$_2$ groups to nitrogen atoms. Green boxes: protons from aliphatic chains.
Top: iNDI spectra after 30 minutes of milling at RT.
Bottom: NDI spectra after a few minutes of heating in solution at 130°C.

With this positive result in hand, it was necessary to transfer these high temperature conditions to the ball mill environment. Several parameters were then modified following the study of Schmidt *et al.* who investigated the temperature progression in a mixer ball mill.[99] Indeed, his group found that by increasing the volume of the jars and the number of milling balls while decreasing the milling load, the temperature could be dramatically increased (up to 80°C at the outer surface of the jars, according to real-time measurements). Therefore, it was decided to rerun the reaction in a bigger stainless steel grinding jar (50 mL), which could accommodate a greater number of milling balls (4x10 mm + 4x12 mm + 4x15 mm diameter), whilst reducing the milling load but maintaining a milling frequency of 30 Hz for 90 minutes.

As discussed in introduction, decreasing the milling load allows the milling balls to have more room in the jars, reducing damping between the balls and the jar, and thus generating more thermal energy. Indeed, when applying the previous parameters and reducing the milling load from 20 units (which is the usual recommended value) to 8.5 mg.mL^{-1}, the external temperature of the milling jars increased to approximately 70°C according to infrared measurements. As far as we know, it is still not possible to measure the temperature inside the jars, as any type of electronical device would be crushed by the milling balls during the run. However, some groups have much improved the way to control the temperature during a mechanochemical milling reaction.[100] The desired NDI was afforded as a pink powder in quantitative yield (Table 5, entry 1) after the crude product was collected with dichloromethane, filtered, and concentrated by rotary evaporation.

Subsequently, the scope of the reaction was studied by attempting to synthesise a series of 5 NDI-based systems which varied by the structure of the amine residue added.

Table 5. *Series of NDI-based scaffolds synthesised by mechanochemistry and in solution.*
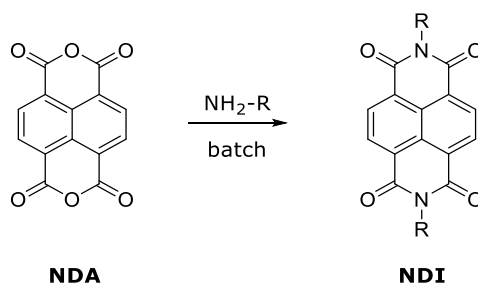
| Entry | R-NH$_2$ group | | MC^a Yield | SB^b Yield |
	Name	Equiv.	(%)	(%)
1	2-ethylhexylamine	2	quant.	Not attempt.
2	aniline	2	42^c	Not attempt.
3	benzylamine	2	78	Not attempt.
4	naphthalamine	2	low^c	88
5	octadecylamine	2	low^c	88

^{a} Mechanochemical conditions: VBM 30 Hz, stainless steel grinding jar (50 mL), stainless steel milling ball(s) (8-14 x 12 mm diam.); neat; milling load = 8.5 mg.mL^{-1}; time = 90 min; proportions and yields are given.
^{b} Solvent-based conditions: reflux in dry DMF for 16 h under argon atmosphere; proportions and yields are given.
^{c} Desired NDI was formed but in small quantities, most of the crude being a black insoluble solid.

According to the values from Table 5, these mechanochemical parameters showed promising results towards the preparation of NDIs in 100% solvent-free conditions in a ball mill. However, they are not always the best conditions in some cases (Table 5, entries 2, 4 and 5), as still a lot of insoluble material is formed and removed by a filtration over celite, affording non-quantitative yields. No improvement was observed when a small excess of amine (2.5 equivalents) was used. Yields correspond to the molar ratio of the target product to starting material as determined by ^{1}H NMR spectroscopy. Also, for three other amine groups (Table 5, entries 4 to 6), the desired products were not observed. This is probably due to an inner temperature which is still not enough to complete the ring closing step, as described previously (Figure 12). Despite this outcome, their synthesis in solution-based conditions was successfully achieved, affording yields of 88% when either using naphthalamine or octadecylamine, while 2-hexyldecanamine was not attempted in solution.

These experiments have shown for the first time it is possible to synthesis NDI-based products by mechanochemistry. Therefore, we decided to move

on to investigate the bromination of NDA (Scheme 7, route i.) as discussed in the following section.

2.1.2.   Synthetic investigations into NDA bromination

In order to perform a selective bromination reaction on highly conjugated polyaromatic starting materials such as NDA, several solution state methodologies are described in the literature. The lack of a universal method to produce this value molecule suggests that the synthesise is difficult to reproduce (Table 3). Many of these synthesise use dibromoisocyanuric acid (DBCA) or dibromodimethylhydantoin (DBDMH) as brominating agent.

Because of the capricious nature of this reaction, when designing the first synthesis in the solid state, we thought useful to also try with two other agents (Scheme 8, bottom): tribromoisocyanuric acid (TBCA) and *N*-bromosuccinimide (NBS), alongside the standard reagents as will be presented further in this section.
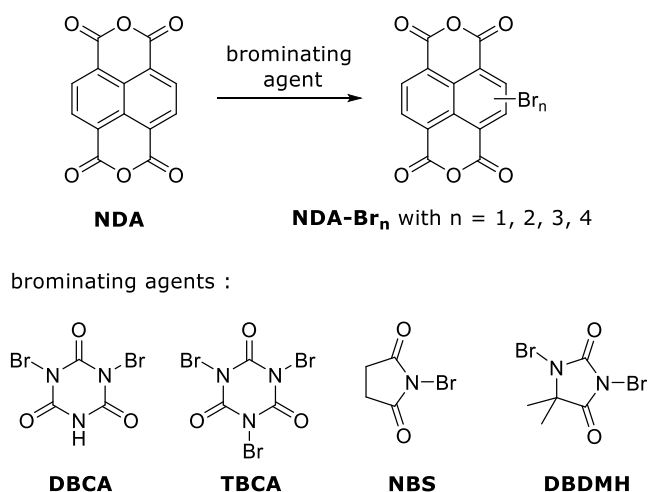
Scheme 8. *Top: NDA bromination step. Bottom: Different brominating agents investigated.*

To provide a starting point for our synthesis, we were inspired by the work of Chaignon *et al.*[65] They reported the dibrominated compound NDA-Br$_2$ (Scheme 7, route i.) could be accessed by the addition of two equivalents of DBCA to NDA in concentrated sulphuric acid at 130°C for 15 hours, then imidisation in acetic acid at 130°C for one hour, affording the desired product in 28% overall yield. Therefore, this was selected as a good starting point for this study.

Initially, two different ranges of mechanochemical conditions were studied to try to observe the bromination of NDA in the solid-state for the first time. The preliminary range of condition (Table 6, MC 1, entries 1 to 17) were selected in the first instance to be typical low energy mechanochemistry parameters (specific details can be found at the bottom of Table 6) to investigate the synthesis under mild conditions. At the start of the optimisation procedure, varying equivalences of DBCA and milling times were trying, while working under neat or sulfuric acid LAG conditions (Table 6, entries 1, 2, 3, 4, 5). One ^{1}H NMR singlet peak was expected at 8.78 ppm,[101] corresponding to NDA-Br$_2$, while two doublets at 8.21 and 8.58 ppm[101] would mean that the mono-brominated NDA was formed (Figure 13).
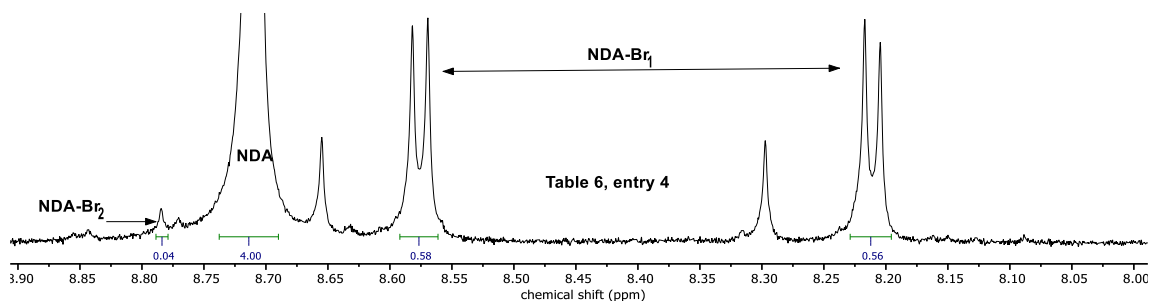
Figure 13. ^{1}H NMR spectra of brominated NDA.

This led to low conversions, up to 17% conversion after 180 minutes milling time, based on ^{1}H NMR spectroscopy (Table 6, entry 4).

In the meantime, two attempts were conducted using a widely used and inexpensive brominating agent: NBS. Unfortunately, almost no conversion was observed (Table 6, entries 6 and 7). Then, it was decided to replace sulfuric acid by oleum, which is a solution of sulphur trioxide in sulfuric acid (Table 6, entries 8 to 17). Slightly better conversions were observed, and the best conditions found for producing single isomeric product were by using 1.4 equivalents of dibromodimethylhydantoin (DBDMH) as brominating agent, oleum as liquid additive, for 180 minutes, which resulted in almost 50% yield of NDA-Br$_2$ (Figure 14 and Table 6, entry 17).
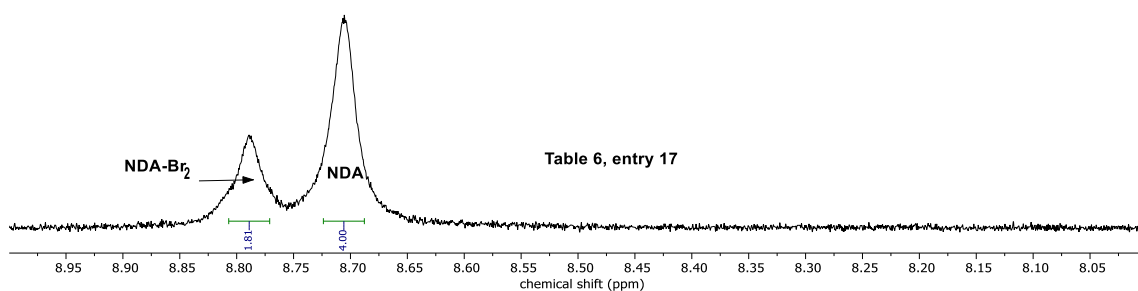
Figure 14. ¹H NMR from Table 6, entry 17.

The conditions that led to full conversions of starting material NDA were when at least 2 equivalents of DBCA as brominating reagent were used, oleum as liquid additive, and for 180 minutes (Table 6, entries 13 to 15). However, these conditions resulted in the formation of mostly NDA-Br$_3$ and almost certainly NDA-Br$_4$ (Figure 15). Indeed, one must pay attention to the presence of product NDA-Br$_4$ as it is not detectable via ¹H NMR spectroscopy and even traces of this product would alter the NMR-based estimation of the percentages given.
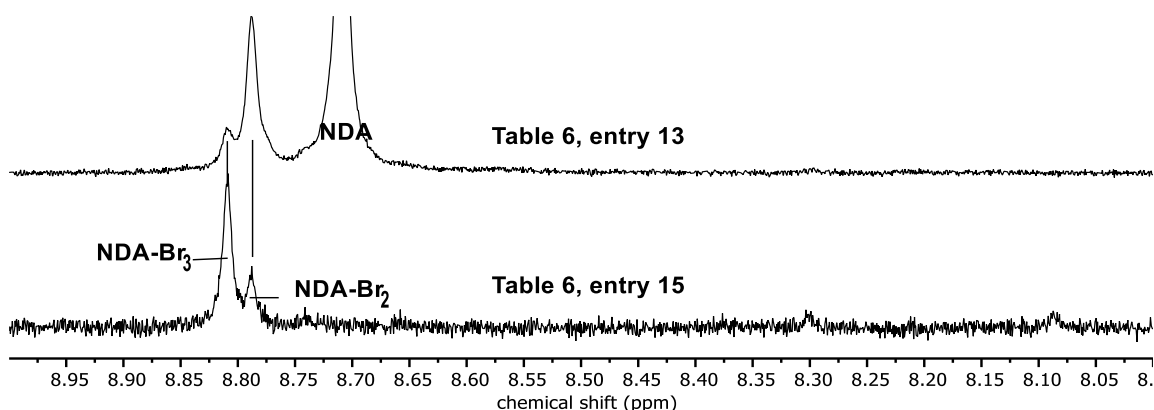
Figure 15. ¹H NMR spectra of brominated NDAs.

When concentrated sulphuric acid was used as liquid additive in place of oleum (Table 6, entries 3 to 7, 16 and 22), very low conversions were observed, even after 180 minutes.

Finally, observations from the first range of condition led to change the mechanochemical parameters, with the aim of increasing the temperature and perhaps, decreasing the reaction time while reaching full conversion and satisfying selectivity. Moreover, this second range of conditions (Table 6, MC 2, entries 18 to 22) were conducted using DBDMH only, as it was considered to be the best agent to avoid the formation of NDA-Br$_1$ and NDA-Br$_3$. This strategy was confirmed when nearly full conversion was reached in only 90

minutes (Table 6, entries 19 to 21). However, first attempts afforded the dibrominated product but also some impurities (Figure 14, top spectra), that could have been eliminated by increasing the milling load (and hence decreasing the temperature; Table 6, entry 21), and by conducting a recrystallization from DMF.
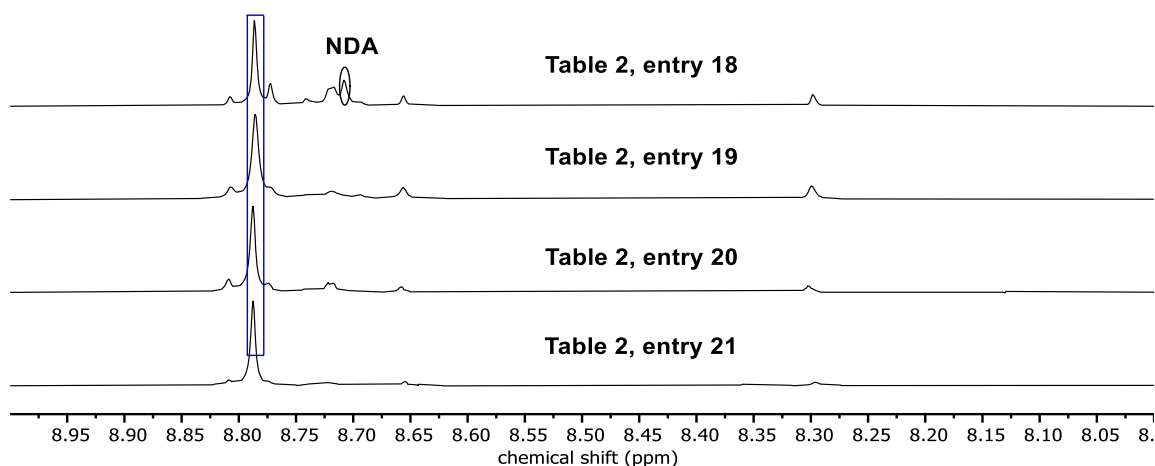
Figure 16. *¹H NMR spectra of brominated NDAs. NDA-Br₂ peaks are circled in blue.*

This optimisation is an important result for two reasons: First, it was possible to precisely detail the composition and characterise the brominated NDAs formed while, as mentioned in the introduction, most publications[79] report using the crude without further characterisation, which can lead to poor yields or selectivity issues in the further steps because the crude is indeed a mixture of *n*-brominated NDAs (n = mono, di, tri, tetra, scheme 8). Secondly, this is the first example showing such results using only a ball mill under almost solvent-less conditions. The complete study can be found in the following Table 6.

Table 6. *Study of the mechanosynthesis of brominated NDAs (Scheme 2, route i.).*

Entry	Brom. agent		LAG	ML^a	MC^b	Time (min)	¹H NMR molar % of			
	Name	Equiv.					NDA	NDA-Br$_1$	NDA-Br$_2$	NDA-Br$_3$
1	DBCA	1	Neat	20	1	90	100	0	0	0
2	DBCA	2	H$_2$SO$_4$	20	1	90	96	4	0	0
3	DBCA	2	H$_2$SO$_4$	20	1	180	90	3	7	0
4	DBCA	3	H$_2$SO$_4$	20	1	180	83	15	2	0
5	DBCA	5	H$_2$SO$_4$	20	1	90	88	2	10	0
6	NBS	2	Neat	20	1	90	100	0	0	0
7	NBS	2	H$_2$SO$_4$	20	1	90	95	5	0	0
8	DBCA	1.4	oleum	20	1	180	17	0	49	34
9	TBCA	0.5	oleum	20	1	180	76	0	24	0
10	DBCA	0.5	oleum	20	1	180	75	2	15	7

| Entry	Brom. agent		LAG	ML[a]	MC[b]	Time (min)	^{1}H NMR molar % of			
	Name	Equiv.					NDA	NDA-Br$_1$	NDA-Br$_2$	NDA-Br$_3$
11	DBCA	1	oleum	20	1	180	49	0	32	19
12	DBCA	1	oleum	20	1	360	48	0	35	18
13	DBCA	2	oleum	20	1	180	0	0	16	84
14	DBCA	2	oleum	20	1	360	0	0	16	84
15	DBCA	3	oleum	20	1	180	0	0	0	?[c]
16	DBDMH	1.4	H$_2$SO$_4$	20	1	90	100	0	0	0
17	DBDMH	1.4	oleum	20	1	180	51	0	49	0
18	DBDMH	1.4	oleum	8.5	2	90	12	0	72	16
19	DBDMH	1.6	oleum	8.5	2	90	0	0	81	19
20	DBDMH	1.6	oleum	10	2	90	0	0	79	21
21	DBDMH	1.6	oleum	20	2	90	0	0	89	11
22	DBDMH	1.4	H$_2$SO$_4$	20	2	90	95	0	5	0

[a] ML (mg.mL^{-1}) = milling load, defined as the weight of grinding stock divided by the free volume in the grinding jar.
[b] MC = Mechanochemical conditions. Condition 1: VBM 30 Hz, stainless steel grinding jar (10 mL), stainless steel milling ball(s) (1-2 x 10-12 mm diam.); milling loads, proportions, reaction times and conversions are given; total mass of reagents and of liquid additive (LAG): to compute according to milling load. Condition 2: VBM 30 Hz, stainless steel grinding jar (50 mL), stainless steel milling ball(s) (8-14 x 12 mm diam.); milling loads, proportions, reaction times and conversions are given; total mass of reagents and of liquid additive (LAG): to compute according to milling load.
[c] Product NDA-Br$_3$ barely visible by ^{1}H NMR spectroscopy which supposes almost only formation of NDA-Br$_4$.

2.1.3. Imidisation reactions of brominated NDAs

Next, the imidisation of brominated NDA was investigated (Scheme 9) using 2 equivalents of the same 2-ethylhexylamine reagent used previously.
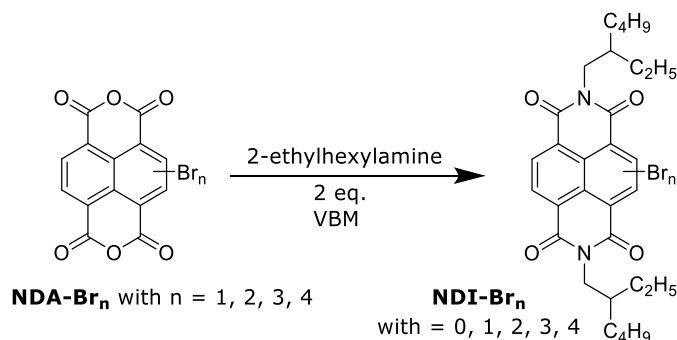
Scheme 9. *Imidisation reaction of brominated NDA.*

For that purpose, a scaled-up NDA bromination reaction was performed in solution, in order to have a large amount of crude material. Following the procedure of Berezin *et al.*,[79] a crude material composed of approximately 62% molar of NDA-Br$_2$ was formed in 15 hours at 50°C, using 1.25 equivalents of DBDMH. This was calculated by ^{1}H NMR spectroscopy considering that NDA possesses 4 protons while NDA-Br$_2$ only 2 protons

(Figure 17). This was used without further purification, considering that a purification after the imidisation step would be easier as the product becomes soluble in common solvents, and can then be purified by standard procedures (recrystallisation/column chromatography).
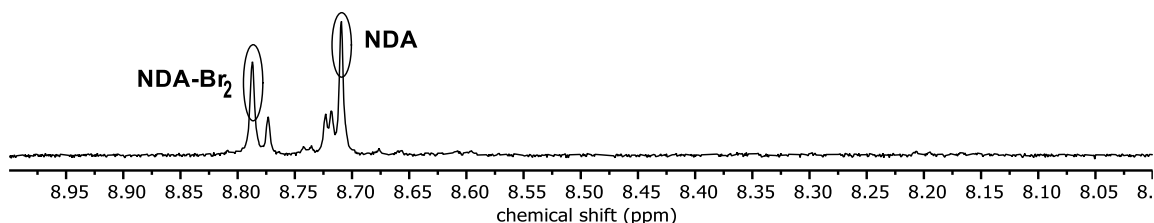

Figure 17. *^{1}H NMR spectra of the large-scaled NDA bromination crude material from solvent-based reaction.*

Following protocol from Guo *et al.*[102], the imidisation step was first realized in a solution of acetic acid at 120°C for 2 hours under argon atmosphere, affording the expected crude mixture composed of the dibrominated NDI but also the non-brominated NDI (Figure 18, spectra a), as a result of the starting material composed of NDA and NDA-Br$_2$. Using the same rationale for analysis of the ^{1}H NMR spectra as outlined above (Figure 17), it is known that NDI contains 4 aromatic protons while NDI-Br$_2$ has only two only aromatic 2 protons. The ratio of NDI:NDI-Br$_2$ calculated is 40:60, which is very similar to the 38:62 ratio from the first step NDA:NDA-Br$_2$. This allows the imidisation reaction conversion to be considered as almost quantitative.

Separation of NDI and NDI-Br$_2$ was achieved because it was found that NDI was significantly soluble in hexane, while NDI-Br$_2$ was not. Thus, simply washing the sample with hexane resulted in rapid purification on a large scale (Figure 18, spectra b). Subsequently, the desired bright yellow dibrominated NDI solid could then be further purified by processing a precipitation from chloroform/hexane (1:3 v/v; Figure 18, spectra c) to give a product that was finally purified by silica gel column chromatography (DCM/hexane; Figure 18, spectra d).
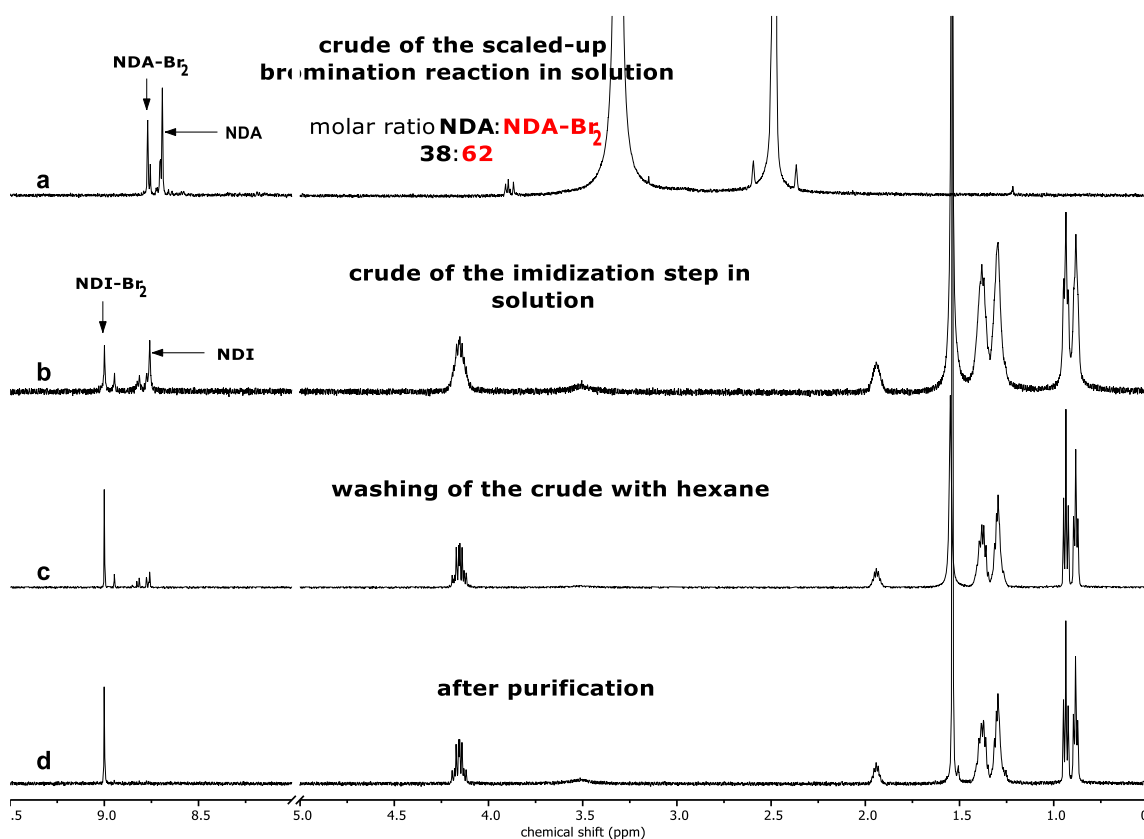
Figure 18. *^{1}H NMR spectra of brominated NDIs in solution.*
a: crude material; b: hexane washing of the crude; c: product from precipitation; d: product from flash chromatography.

With purification procedures established and authentic samples of the products in hand, the imidisation of NDI-Br$_2$ was attempted in the solid-state. Initially this was attempted using the same crude material (NDI:NDI-Br$_2$ ratio 40:60) as previously from the large-scale solvent-based reaction of bromination (Scheme 9).

While respecting the same mechanochemical parameters and workup than previously (Table 6, MC 2), with a milling load of 13.5 mg.mL^{-1}, 2 equivalents of amine, and with acetic acid as liquid additive, a non-expected crude material was obtained after 60 minutes of milling. Indeed, almost only NDI was visible by ^{1}H NMR spectroscopy (Figure 19 and Figure 20, middle spectra) while NDI-Br$_2$ was barely formed (molar ratio NDI:NDI-Br$_2$ = 82:**18**), by comparison with the crude from the solvent-based reaction (molar ratio NDA:NDA-Br$_2$ = 38:**62**).

Figure 19. *^{1}H NMR spectra of brominated NDI.*

At that point, three assumptions were made:
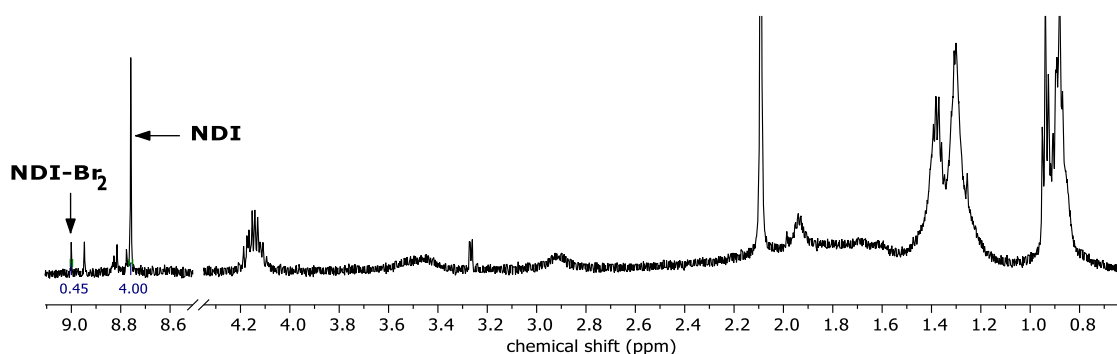
- NDA-Br$_2$ needs higher temperature than NDA to complete the ring closing step, meaning that the reaction was not fully completed. This hypothesis could explain the presence of broad singlets between 2.5 and 4.0 ppm, more visible in the solid-state than in solution (Figure 19).

- NDA-Br$_2$ or NDI-Br$_2$ are unstable to mechanical energy in the solid-state, and were widely decomposed into NDA or NDI, resulting in a large excess of NDI at the end of the imidisation.

- NDA-Br$_2$ or NDI-Br$_2$ are unstable to mechanical energy in the solid-state, and the substitutions occurred, not only at the dianhydride locations, but also at the two bromines.

Even though no excess of amine was used for this work, the latter two speculations are strengthened by two reactions reported in the literature that were also conducted in highly energetic conditions using a microwave, and with an excess of amine. The first one[103] shows that the tetra-substituted NDI can be formed in only 2 minutes, while the second one[104] shows a crude mixture of the same tetra-substituted NDI but also the tri-substituted NDI (one bromine being substituted by a hydrogen) in 15 minutes (Scheme 10).
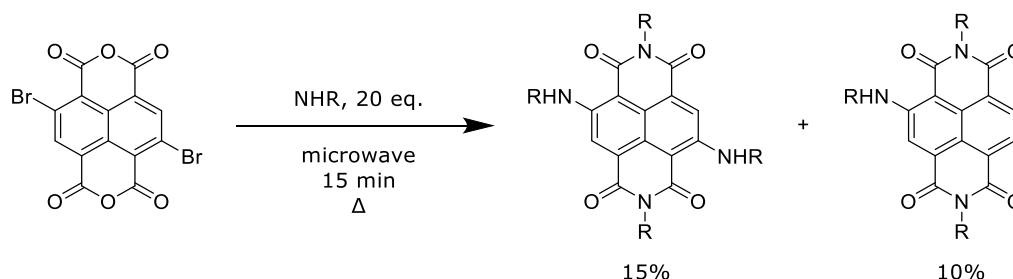
Scheme 10. *Example of the result of NDA-Br$_2$ imidisation in a microwave*

In order to investigate the validity of our first hypothesis, a new methodology was attempted to try to reach even higher temperatures inside the grinding jars during a mechanochemical reaction. It consisted in preheating the opened jars in an oven at 130°C overnight before adding the reagents. After 90 minutes of milling, the closed jars are heated again at 160°C for 45 minutes before to run the milling again for 60 minutes. For this method, grinding jars composed of hardened steel were used, as its thermal conductivity is better than stainless steel. However, those jars being smaller with an internal volume of 25 mL, therefore, only 2 milling balls were used, compared to the 13 balls used in 50 mL jars. Because of this, the temperatures measured after the milling times were only 40°C even if the jars were preheated at much higher temperatures. This observation was unexpected and would mean that the inner temperature is not constantly at the high value during the milling. Indeed, no significant difference was observed between the pre-heated or non-pre-heated methods described for the solid-state – both gave crude products containing only about 13% of NDI-Br_2 (Figure 20, middle and bottom spectra).
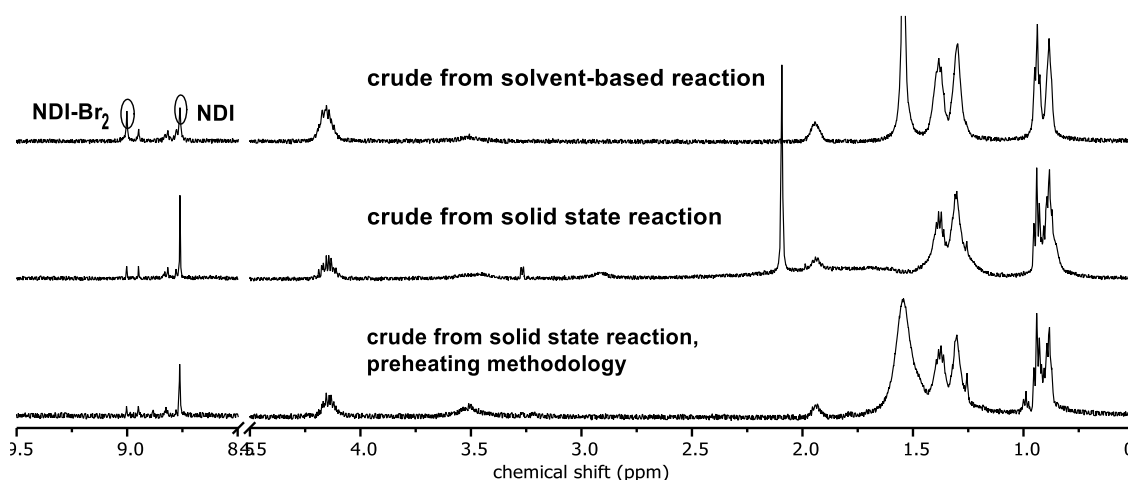
Figure 20. ^1H *NMR spectra of brominated NDIs in solution and the solid-state.*

Finally, the last route to synthesise NDI-Br_2 from NDI was investigated (Scheme 7, route iv.), which is the one performing the bromination step *after* the imidisation. This reaction was only attempted in the solid-state, using the 2-ethylhexylamine-NDI also synthesised in the solid-state, 1.8 equivalents of DBDMH as brominating agent, and oleum as liquid additive. Unfortunately, no reactivity was observed after 90 min of grinding at 30 Hz, leaving the starting NDI material almost completely recoverable.

2.1.4.   Cross-coupling reactions of brominated NDIs

This final section is about the last steps necessary to isolate NDI-based polymers. Different routes are highlighted, but it was decided to focus on the polymerisation of bithiophene NDIs, as it can lead to effective electron acceptors such as N2200 (section X, Scheme 10). We envisaged this could be achieved in two steps in the solid state. Initially to substitute two thiophene groups, then to run the polymerisation in a second step. Prior to starting to make complex polymers, it was decided to target the bithiophene product first. Regarding this substitution, one reaction is often used: the Stille tin coupling, while another methodology is getting more and more considered in the last few years: the C-H activation. Both examples work in presence of a metal catalyst, but the latter does not require tin-based reagents. Stille coupling can theoretically be performing using the 2,5-bis(trimethylstannyl)thiophene, in presence of a palladium(II) catalyst (Scheme 10, top route). Concerning the C-H activation, two options were also imagined: to use the thiophene with NDI-Br$_2$ (Scheme 10, middle route), or to use a di-halogenated thiophene with NDI (Scheme 10, bottom route).
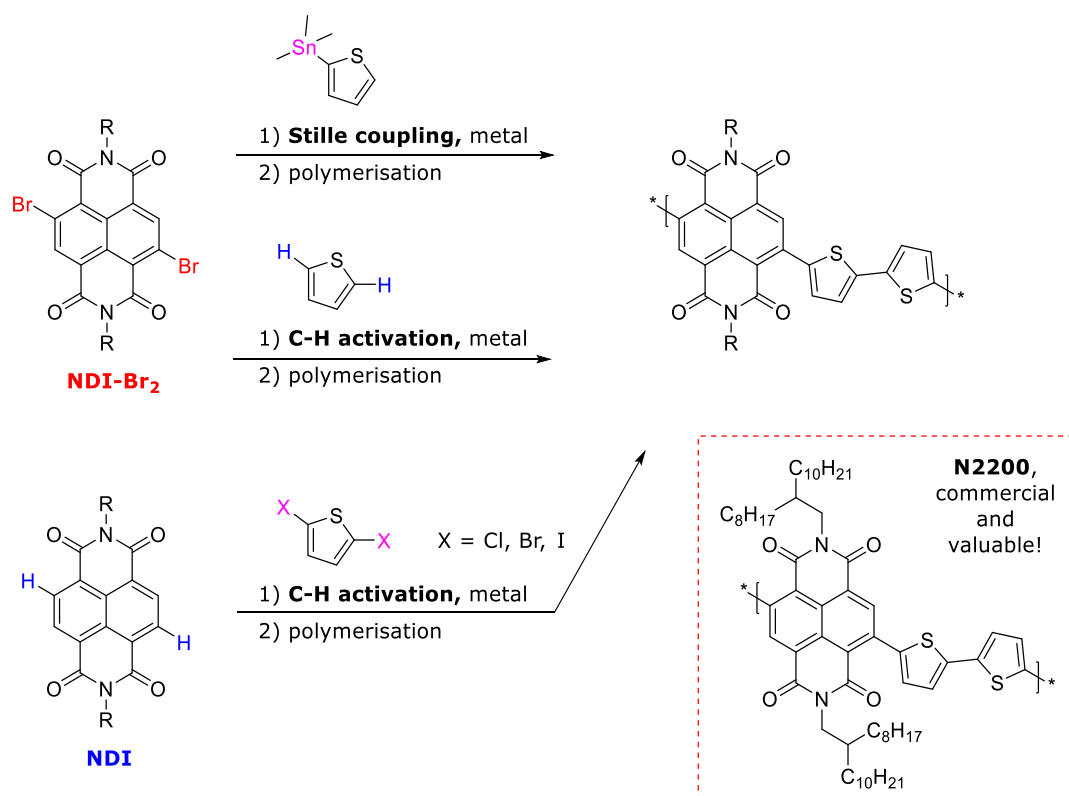
Scheme 11. *Several different routes possible to perform polymerisation of bithiophene from NDI-based material.*

The only route that could be attempted and that will be presented in the further lines is the C-H activation from the NDI-Br$_2$ (Scheme 11, middle route). The two other possibilities could not be investigated within the time available. First, the reaction was performed in solvent-based conditions, in presence of 2-ethylhexylamine-NDI-Br$_2$ from a previous reaction, thiophene, palladium(II) acetate, potassium carbonate, and pivalic acid, in anhydrous toluene, under reflux and for 18 hours. After a common basic workup, and purification on silica gel, the desired product was isolated with a yield of 76%.
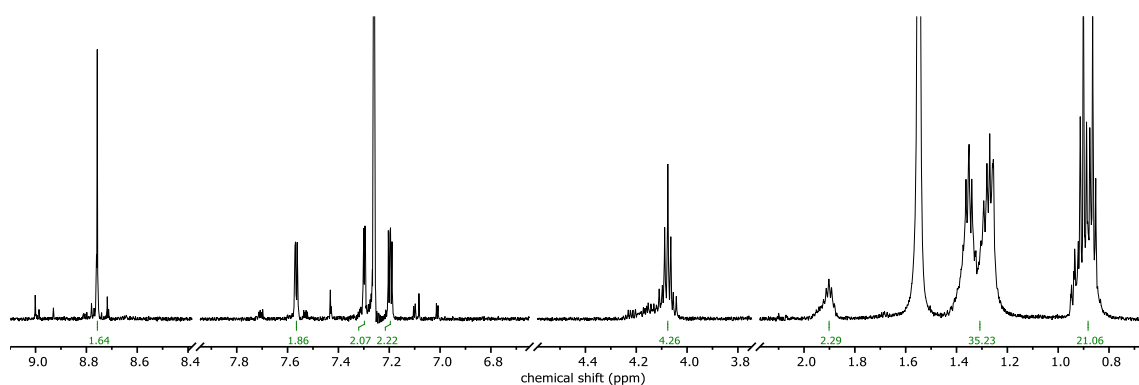

Figure 21. ^{1}H NMR spectra of 2-ethylhexylamine-NDI-dithiophene in solution.

Based on that positive result, the reaction was tried in the solid-state, using the same reagents that in solution, with or without anhydrous toluene as liquid additive, and in a zirconium oxide jar. Unfortunately, after 90 minutes of milling at 30 Hz, the starting material was recovered unchanged, based on ^{1}H NMR. No further investigation could be conducted.

Few months later the work presented in this report, and after some reaction optimisations, promising results were obtained by the group, with the isolation of several NDI derivatives by cross-coupling reactions in the solid-state. At that time, the scope is composed of 10 molecules synthesised from Suzuki-Miyaura reaction, 6 molecules from Sonogashira reaction, and 4 from Buchwald-Hartwig reaction (Appendix 1), with yields from 13 to 83%.

2.2. Mechanochemical synthesis of PMDI derivatives

According to the previous results concerning the preparation of NDI from NDA, a focus turned to the synthesis of PMDI scaffolds from PDCA (Scheme 11). PMDA has a very similar structure to NDA molecules but contained only one central aromatic ring instead of two for NDAs. Although polymers and small molecules containing PDI have been studied for photophysics

applications, they are under-represented in the literature, meaning it is a still open field of investigation for further publications.

Initially we selected to study the synthesis of aniline and benzylamine substituted PDIs (Scheme 11), to compare their reactivity in the solid-state.
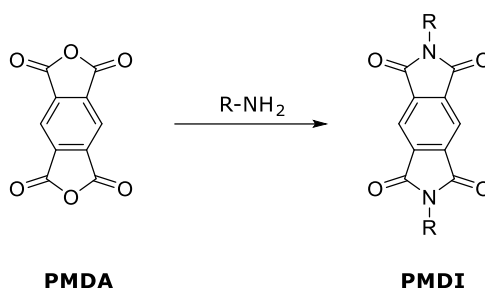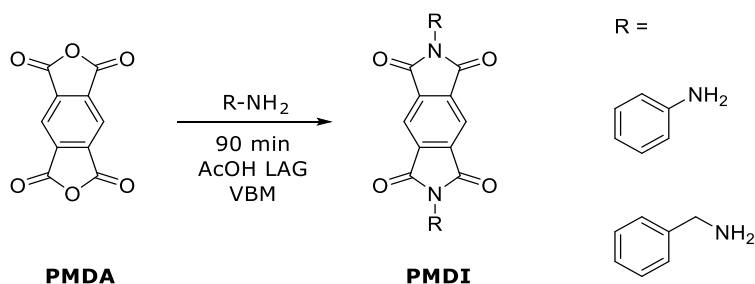

Scheme 12. *Synthetic route to access PMDI scaffolds.*

Again, the solvent-based reactions were first investigated, to allow for optimisation of isolation procedures and provide authentic examples for spectroscopic comparison. Following the work of Smith *et al.*[105] and Ding *et al.*,[106] and as for the synthesis of NDI, high temperatures are required to close the ring system and form the imide structure. Concerning the synthesis of aniline-PMDI, only one preparation is referred in the literature,[107] describing five steps from 2,5-dihydrothiophene-3,4-dicarboxylic anhydride. Here, its synthesis was achieved in one step from PMDA and aniline, in dry DMF at reflux for two hours under argon atmosphere. When the solution of DMF was cooled down to room temperature, pale yellow crystals formed from the solution, yielding 79% of pure aniline-PMDI without any further purification (according to elemental analyses, as the product could not be dissolved in any common solvent). Benzylamine-PMDI, was similarly prepared with the addition of 3 equivalents of benzylamine to PMDI, in acetic acid at reflux for three hours. The pure product was isolated in 42% yield as colourless crystals after a recrystallization from ethanol.

Scheme 13. *Synthetic route to access PMDI scaffolds in the solid-state.*

Next, the synthesis of PDI derivatives was studied for the first time in the solid-state (Scheme 12). It was decided, in a first instance, to use benzylamine as the corresponding product is soluble in chloroform, thus easier to characterise by ^{1}H NMR spectroscopy. Conducting the reaction is 50 mL steel jar with 8 steel grinding balls in neat conditions, it was found that the temperature did not exceed 35°C at the outer surface of the jar after 90 minutes of milling. This lack of heat prevented again the ring closing step to occur (as observed for the NDI example in Figure 12). However, when a very small amount of acetic acid was added in the jar as liquid additive, temperature reached over 80°C after 90 minutes, letting the first traces of desired product appearing by ^{1}H NMR spectroscopy. Finally, a recrystallization from ethanol afforded the pure product with a yield of 19% (Figure 22).
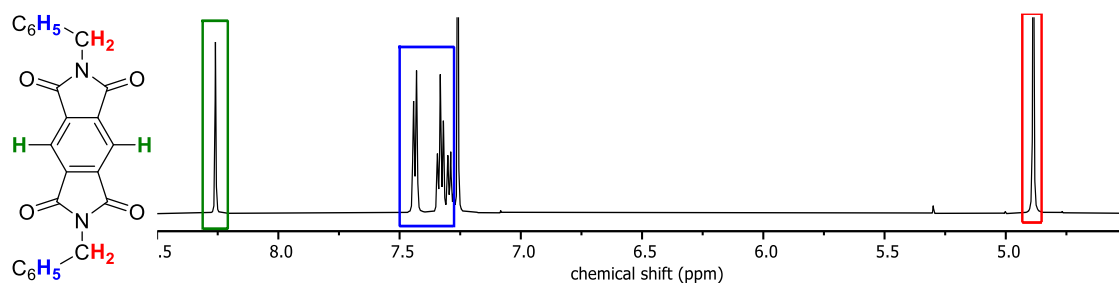

Figure 22. ^{1}H NMR spectra of benzylamine-PMDI with protons identified by colour.

3. CONCLUSION AND FUTURE WORK

This research has investigated the synthesis of highly conjugated compounds such as NDI or PMDI in the solid-state. These molecules were selected as they are amongst the best electron acceptors for organic solar cells. Specifically, this report has produced two significant discoveries that will be of benefit to all the future work regarding the production of NDI-based organic photovoltaics by mechanochemistry.

The first discovery concerns the bromination reaction of NDA in the solid-state that was described at full conversion and with a better selectivity in dibrominated NDA than what can be found in the literature in solvent-based condition. The reaction optimisation was particularly tedious but led, after an extensive survey of conditions, to excellent molar ratio of NDA:NDA-Br$_2$, even assuming no NDA-Br$_4$ is present in the product mix.

The second one is about the imidisation reaction of NDA, which was more manageable than the bromination step. Most of the reported reactions in solution are performed at high temperature for several hours in DMF or concentrated acids. In contrast, in this thesis we presented mechanochemical synthesis of NDI and PMDI in 90 or less minutes and with never more than 770 µL of solvent (when not solvent-free) whilst achieving quantitative or very good yields. For that purpose, it was confirmed that high temperatures are absolutely required in the ring closing step to the formation of NDI and PMDI. Although a planetary ball mill would have been a more appropriate alternative, such temperatures could also be reached in a mixer ball by forcing the mechanochemical parameters to an extreme. These conditions were successful to synthesise four NDI scaffolds in the solid-state but still insufficient when having dibrominated NDA as starting material, and despite attempting a range of conditions, which are still being optimized.

Another part of the work focused on the study of the different pathways leading to the polymers of interest. One type of reaction was particularly challenging: the cross-coupling C-H activation. Naturally, more and more synthetic chemists try to trend towards those methodologies in order to eventually avoid some complicated halogenation steps.[108,109] A few teams have now started to investigate the C-H activation by mechanochemistry[110–

[112] which would make the preparation of the polymers much easier and greener (atom and step economy; see the twelve principles of green chemistry[113]). Following the literature, the substituted NDI monomer could be synthesised in solvent-based conditions, but unfortunately, the few experiments tried in the solid-state were not conclusive. Despite these unsuccessful results, we think this methodology is promising and deserve some more work and optimisation to perhaps, be successful.

Since completion of this work several other well-known palladium-catalysed cross-coupling named reactions were identified to be suitable with the formation of the desired substituted NDI derivatives. These are the following: Suzuki-Miyauri coupling, which is the one between organoboronic acid and halides; Stille coupling between stannanes and halides; Sonogashira coupling of terminal alkynes with aryl or vinyl halides; and Buchwald-Hartwig coupling of aryl halides and primary or secondary amines. These reactions were subsequently studied by other members of the group and led to successful results (see Appendix 1).

Finally, in order to have a true idea of the role of temperature in mechanochemical reactions, a new way of measuring it continuously is being explored. According to our research, it could be achieved in a contactless way with the help of an infrared camera or sensor, or with a kind of contact temperature sensor button. Indeed, at the moment, the only way to evaluate it is by stopping the milling and manually measuring it with an infrared laser thermometer at the outer surface of the jars, which is not ideal. Furthermore, on repeated occasions, the reactions described in this report showed that the temperature was often crucial in achieving complete conversion. This technology would bring a huge impact on how the reactions are evolving in the solid-state regarding the temperature parameter.

To summarise, this thesis has reported the solid-state synthesis of brominated NDA and several NDI and PMDI-based scaffolds in the solid-state, which had never been done before. This project could, in a near future and with some additional work, allow to prepare the first organic solar cells by mechanochemistry in the solid-state. This methodology would not only be more environmentally friendly, but also easier and cheaper to design for industrial purposes.

4. EXPERIMENTAL

General procedures

All reagents were purchased from Merck KGaA, Fisher Scientific UK Ltd, Tokyo Chemical Industry UK Ltd, Fluorochem Ltd, and used without further purification. The milling treatments were carried out in a Retsch MM400 vibratory ball mill (VBM) operated at 30 Hz. Milling load is defined as the sum of the mass of the reactants per free volume in the jar. ^{1}H NMR spectra were recorded on Varian VNMRS 500 MHz or 600 MHz spectrometers, at room temperature, using deuterated solvent for calibration (chloroform-d at 7.26 ppm or DMSO-d_6 at 2.50 ppm). ^{13}C NMR analyses were conducted by Rémi Legay from the University of Caen, and spectra recorded on Bruker Avance III 600 MHz spectrometers, at room temperature, using deuterated solvent for calibration (chloroform-d at 77.16 ppm or DMSO-d_6 at 39.52 ppm). Chemical shifts are reported in ppm, usually referenced to TMS as an internal standard, and data reported as s = singlet, d = doublet, t = triplet, q = quadruplet, qt = quintuplet, sept = septuplet, m = multiplet; integration. Mass spectrometry (MS) analyses were conducted by Dr Abdul-Sada. ESI mass spectra were obtained using a Bruker Daltonics Apex III, using Apollo ESI as the ESI source; EI mass spectra were obtained using a Fissions VG Autospec instrument used at 70 eV. Melting points (MP) were determined using a Stanford Research Systems Optimelt and were uncorrected. Elemental analyses (EA) were conducted by Mr Stephen Boyer from the London Metropolitan University, using a Thermo Scientific Flash 2000 machine.

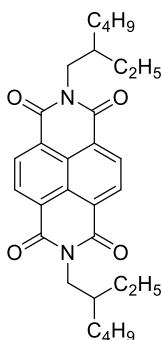### 2,6-dibromo-1,4,5,8-naphthalenetetracarboxylic acid dianhydride
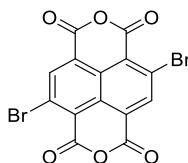
Solvent-based protocol: To a solution of 1,4,5,8-naphtalenetetracarboxylic dianhydride (6 g, 22.38 mmol, 1 equiv.) in sulphuric acid (50 mL) was added 1,3-dibromo-5,5-dimethylhydantoin (8 g, 27.97 mmol, 1.25 equiv.) in four portions over a period of 30 minutes. The resulting mixture was stirred at

80°C for 15 hours in a sealed flask. The reaction mixture was poured onto ice and the resulting precipitate was slowly filtered on a low porosity sintered frit, washed with water and methanol, and dried overnight in a vacuum oven to afford a bright yellow solid composed of the desired dibromo- product (62% by moles, 72% by weight), and as by-product: the starting material (38% by moles, 28% by weight), according to ^{1}H NMR. Because of poor solubility in any usual solvent, the crude product was used without further purification. **^{1}H NMR** (600 MHz, DMSO-d_6) δ = 8.79 (s, 2H, H$_{arom.}$).

Solid-state protocol: In one step, 1,4,5,8-naphtalenetetracarboxylic dianhydride (0.494 mmol, 1 equiv.), and 1,3-dibromo-5,5-dimethylhydantoin (0.791 mmol, 1.6 equiv.) were introduced in a 50 mL stainless steel grinding jar with 8 stainless steel balls (12 mm diameter) and 770 µL of oleum as liquid additive. Total mass of the reagents was calculated so that milling load equals 20 mg.mL^{-1}. The jar was closed and subjected to grinding for 90 minutes in the VBM operated at 30 Hz. **Beware**: toxic bromine red fumes might be released when opening the vessel. Inside the jar was directly poured ice and water on the resulting yellow oil to precipitate the product. The resulting precipitate was slowly filtered on a low porosity sintered frit, slowly washed with water and methanol, recrystalised from DMF, then dried overnight in vacuum oven to afford a bright yellow thin powder. ^{1}H NMR composition: dibromo- product (89% by moles), and a by-product: the tribromo- product (11% by moles). **^{1}H NMR** (600 MHz, DMSO-d_6) δ = 8.79 (s, 2H, H$_{arom.}$). **MS** (EI) – (m/z) for $C_{30}H_{38}N_2O_4$ calc. 426; found 426.

N,N'-bis(2-ethyl-1-hexyl)naphthalene-1,4,5,8-tetracarboxylic acid diimide

Solid-state protocol: In one step, 1,4,5,8-naphtalenetetracarboxylic dianhydride (0.60 mmol, 1 equiv.), and 2-ethylhexylamine (1.20 mmol, 2

equiv.) were introduced in a 50 mL stainless steel grinding jar with 12 stainless steel balls (12 mm diameter). Total mass of the reagents was calculated so that milling load equals 10 mg.mL^{-1}. The jar was closed and subjected to grinding for 90 minutes in the VBM operated at 30 Hz. The resulting solid was collected by dissolving it with the minimum amount of dichloromethane, filtered over celite and the filtrate concentrated by rotary evaporation to afford the desired product as a salmon solid (quant. yield). **^{1}H NMR** (600 MHz, chloroform-d) δ = 8.76 (s, 4H, H$_{arom.}$), 4.15 (qd, 4H, R-CH$_2$-CH-(CH$_2$)$_n$-CH$_3$), 1.97–1.90 (m, 2H, R-CH$_2$-CH-(CH$_2$)$_n$-CH$_3$), 1.41–1.26 (m, 16H, R-CH$_2$-CH-(CH$_2$)$_n$-CH$_3$), 0.94 (t, 6H, J = 7.4 Hz, R-CH$_2$-CH-(CH$_2$)$_n$-CH$_3$), 0.88 (t, 6H, J = 6.9 Hz, R-CH$_2$-CH-(CH$_2$)$_n$-CH$_3$). **^{13}C NMR** (151 MHz, chloroform-d) δ = 163.6, 131.4, 127.1, 127.0, 77.6, 77.4, 77.2, 45.0, 38.3, 31.1, 29.0, 24.4, 23.4, 14.4, 11.0. **MS** (EI) – (m/z) for C$_{30}$H$_{38}$N$_2$O$_4$ calc. 490; found 490. **MP**: 199.5-200.5°C. **EA** for C$_{30}$H$_{38}$N$_2$O$_4$ calc. C, 73.44; H, 7.81; N, 5.71; found C, 73.24; H, 7.76; N, 5.61.

N,N'-bis(2-hexyl-1-octyl)naphthalene-1,4,5,8-tetracarboxylic acid diimide
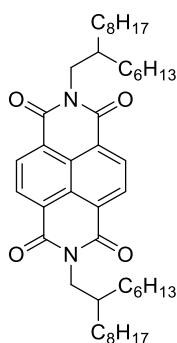
Solid-state protocol: In one step, 1,4,5,8-naphtalenetetracarboxylic dianhydride (0.55 mmol, 1 equiv.), and 2-hexyloctylamine (1.10 mmol, 2 equiv.) were introduced in a 50 mL stainless steel grinding jar with 12 stainless steel balls (12 mm diameter). Total mass of the reagents was calculated so that milling load equals 10 mg.mL^{-1}. The jar was closed and subjected to grinding for 90 minutes in the VBM operated at 30 Hz. The resulting solid was collected by dissolving it with the minimum amount of dichloromethane, filtered over celite and the filtrate concentrated by rotary evaporation to afford the desired product as a dark red oil. **^{1}H NMR** (600 MHz, chloroform-d) δ = 8.76 (s, 4H, H$_{arom.}$), 4.14 (qd, 4H, J = 7.3 Hz, R-CH$_2$-

CH-(CH$_2$)$_n$-CH$_3$), 2.02–1.96 (m, 2H, R-CH$_2$-CH-(CH$_2$)$_n$-CH$_3$), 1.32–1.19 (m, 48H, R-CH$_2$-CH-(CH$_2$)$_n$-CH$_3$), 0.86–0.82 (m, 12H, R-CH$_2$-CH-(CH$_2$)$_n$-CH$_3$). **^{13}C NMR** (151 MHz, chloroform-*d*) δ = 163.4, 131.2, 126.9, 126.7, 77.37, 77.2, 76.9, 45.1, 36.8, 32.0, 32.0, 31.8, 31.8, 30.1, 29.8, 29.7, 29.4, 26.6, 26.6, 22.8, 22.8, 14.2. **MS** (EI) – (m/z) for C$_{46}$H$_{70}$N$_2$O$_4$ calc. 715; found 715. **EA** for C$_{46}$H$_{70}$N$_2$O$_4$ calc. C, 77.27; H, 9.87; N, 3.92; found C, 77.18; H, 9.58; N, 3.83.

**N,N'-bis(phenyl)-1,4,5,8-naphthalenebis(dicarboximide)**
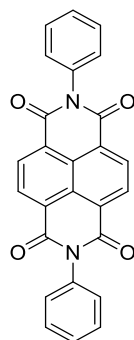
Solid-state protocol: In one step, 1,4,5,8-naphtalenetetracarboxylic dianhydride (0.70 mmol, 1 equiv.), and aniline (1.4 mmol, 2 equiv.) were introduced in a 50 mL stainless steel grinding jar with 12 stainless steel balls (12 mm diameter). Total mass of the reagents was calculated so that milling load equals 10 mg.mL^{-1}. The jar was closed and subjected to grinding for 90 minutes in the VBM operated at 30 Hz. The resulting solid was collected by dissolving it with the minimum amount of dichloromethane, filtered over celite and the filtrate concentrated by rotary evaporation to afford the desired product as bronze needles (124.1 mg, 42%). **^{1}H NMR** (600 MHz, DMSO-*d$_6$*) δ = 8.73 (s, 4H, H$_{arom.}$), 7.57 (t, 4H, H$_{Ph}$), 7.50 (t, 2H, *J* = 6.7, 1.3 Hz, H$_{Ph}$), 7.47 (d, 4H, H$_{Ph}$). **^{13}C NMR** (151 MHz, DMSO-*d$_6$*) δ = 163.0, 135.6, 130.5, 129.0, 129.0, 128.5, 127.0, 126.7. **MS** (EI) – (m/z) for C$_{26}$H$_{14}$N$_2$O$_4$ calc. 418; found 418. **MP**: >400°C. **EA** for C$_{26}$H$_{14}$N$_2$O$_4$ calc. C, 74.64; H, 3.37; N, 6.70; found C, 74.53; H, 3.43; N, 6.54.

N,N'-bis(phenylmethyl)naphthalene-1,4,5,8-tetracarboxylic diimide
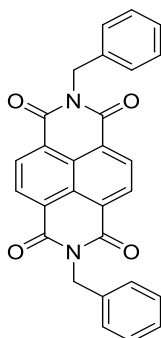
Solid-state protocol: In one step, 1,4,5,8-naphtalenetetracarboxylic dianhydride (0.66 mmol, 1 equiv.), and benzylamine (1.32 mmol, 2 equiv.) were introduced in a 50 mL stainless steel grinding jar with 12 stainless steel balls (12 mm diameter). Total mass of the reagents was calculated so that milling load equals 10 mg.mL^{-1}. The jar was closed and subjected to grinding for 90 minutes in the VBM operated at 30 Hz. The resulting solid was collected by dissolving it with the minimum amount of dichloromethane, filtered over celite and the filtrate concentrated by rotary evaporation to afford the desired product as a pale orange solid (227.6 mg, 78%). **^{1}H NMR** (600 MHz, DMSO-d_6) δ = 8.71 (s, 4H, H$_{arom.}$), 7.40 (d, 4H, H$_{Ph}$), 7.31 (t, 4H, H$_{Ph}$), 7.25 (t, 2H, J = 7.3, 1.5 Hz, H$_{Ph}$), 5.28 (s, 4H, R-CH$_2$-Ph). **^{13}C NMR** (151 MHz, DMSO-d_6) δ = 162.8, 136.9, 130.7, 128.4, 127.6, 127.2, 126.4, 126.4, 43.4. **MS** (EI) – (m/z) for C28H18N2O4 Calc. 446; Found 447. **MP**: 261.5-263.5°C. **EA** for C28H18N2O4 Calc. C, 75.33; H, 4.06; N, 6.27; Found C, 75.09; H, 4.00; N, 5.85.
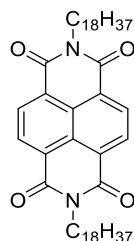
2,7-Bis(1-naphthyl)benzo[lmn][3,8]phenanthroline-1,3,6,8-tetrone
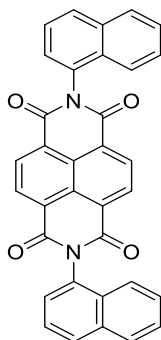
Solvent-based protocol: To a solution of 1,4,5,8-naphtalenetetracarboxylic dianhydride (1.8 mmol, 1 equiv.) in dry DMF (5 mL) was added 1-naphthylamine (3.6 mmol, 2 equiv.) in one portion. The resulting mixture was stirred at reflux for 15 hours under argon atmosphere. The reaction

mixture was cooled to room temperature and the resulting precipitate was filtered, washed with methanol and hexane, and dried overnight in vacuum oven to afford the desired product as a yellow solid (827.0 mg, 88%). **¹H NMR** (600 MHz, DMSO-d_6) δ = 8.78 (s, 4H, H$_{arom.}$), 8.12 (dd, 4H, J = 17.6, 8.1 Hz, H$_{naph.}$), 7.96 (d, 2H, J = 8.5 Hz, H$_{naph.}$), 7.76–7.69 (m, 4H, H$_{naph.}$), 7.61 (t, 2H, J = 7.4 Hz, H$_{naph.}$), 7.51 (t, 2H, J = 8.4, 6.7 Hz, H$_{naph.}$). **¹³C NMR** (151 MHz, DMSO-d_6) δ = 163.0, 133.9, 130.7, 129.1, 128.3, 127.0, 126.4, 125.8, 125.2, 123.1, 40.0, 39.9, 39.9, 39.8, 39.8, 39.7, 39.5, 39.4, 39.2, 39.1. **MS** (EI) – (m/z) for $C_{34}H_{18}N_2O_4$ calc. 518.13; found 518. **EA** for $C_{34}H_{18}N_2O_4$ calc. C, 78.76; H, 3.50; N, 5.40; found C, 78.59; H, 3.28; N, 5.39.

N,N′-bis(octadecyl)-1,4,5,8-naphthalenebis(dicarboximide)

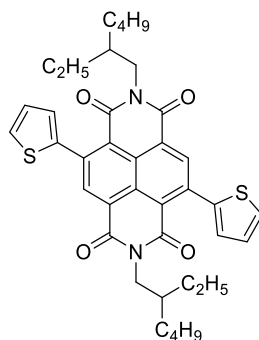
Solvent-based protocol: To a solution of 1,4,5,8-naphtalenetetracarboxylic dianhydride (1.24 mmol, 1 equiv.) in dry DMF (5 mL) was added octadecylamine (2.48 mmol, 2 equiv.) in one portion. The resulting mixture was stirred at reflux for 15 hours under argon atmosphere. The reaction mixture was cooled to room temperature and the resulting precipitate was filtered, washed with methanol and hexane, and dried overnight in vacuum oven to afford the desired product as a grey solid (837.7 mg, 88%). **¹H NMR** (600 MHz, chloroform-d) δ = 8.76 (s, 4H, H$_{arom.}$), 4.19 (t, 4H, J = 8.9, 6.5 Hz, R-(CH$_2$)$_n$-CH$_3$), 1.75 (m, 4H, J = 7.6 Hz, R-(CH$_2$)$_n$-CH$_3$), 1.45–1.39 (m, 4H, R-(CH$_2$)$_n$-CH$_3$), 1.38–1.34 (m, 4H, R-(CH$_2$)$_n$-CH$_3$), 1.23 (m, 52H, R-(CH$_2$)$_n$-CH$_3$), 0.88 (t, 6H, J = 6.9 Hz, R-(CH$_2$)$_n$-CH$_3$). **¹³C NMR** (151 MHz, chloroform-d) δ = 163.0, 131.1, 126.8, 77.4, 77.2, 76.9, 41.2, 32.1, 29.8, 29.8, 29.8, 29.7, 29.7, 29.5, 29.5, 28.2, 27.2, 22.8. **MS** (EI) – (m/z) for $C_{50}H_{78}N_2O_4$ calc. 771; found 771. **EA** for $C_{50}H_{78}N_2O_4$ calc. C, 77.87; H, 10.20; N, 3.63; found C, 77.93; H, 10.06; N, 3.59.

N,N′-bis(2-ethylhexyl)-2,6-dibromo-1,4,5,8-naphthalenetetracarboxylic acid bisimide
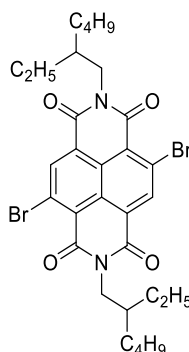
Solvent-based protocol: To a solution of 2,6-dibromo-1,4,5,8-naphthalenetetracarboxylic acid dianhydride (1.59 mmol, 1 equiv.) in acetic acid (15 mL) was introduced an excess of 2-ethylhexylamine (6.36 mmol, 4 equiv.) in several portions with a syringe. The mixture was left to stir and reflux at 120°C for 2 hours under argon atmosphere. The reaction mixture was poured over ice and water and the resulting precipitate was filtered and washed with water, methanol, and hexane to afford a bright pink crude product. The crude was recrystallized from dichloromethane at -20°C. The resulting precipitate is collected on a frit and washed once with cold dichloromethane and hexane to afford the desired product as a pale orange solid. **¹H NMR** (600 MHz, chloroform-d) δ = 9.00 (s, 2H, H$_{arom.}$), 4.16 (qd, 4H, J = 13.0, 7.4 Hz, R-CH$_2$-CH-(CH$_2$)$_n$-CH$_3$), 1.97–1.92 (m, 2H, R-CH$_2$-CH-(CH$_2$)$_n$-CH$_3$), 1.41–1.27 (m, 16H, R-CH$_2$-CH-(CH$_2$)$_n$-CH$_3$), 0.94 (t, 6H, J = 7.4 Hz, R-CH$_2$-CH-(CH$_2$)$_n$-CH$_3$), 0.88 (m, 6H, J = 6.8 Hz, R-CH$_2$-CH-(CH$_2$)$_n$-CH$_3$). **MS (EI)** – (m/z) for C$_{30}$H$_{36}$Br$_2$N$_2$O$_4$ calc. 648; found 648. **EA** for C$_{30}$H$_{36}$Br$_2$N$_2$O$_4$ calc. C, 55.57; H, 5.60; N, 4.32; found C, 55.72; H, 5.39; N, 4.21.

N,N′-bis(2-ethylhexyl)-2,6-di-(2,2′-thienyl)-1,4,5,8-naphthalenetetracarboxylic acid bisimide

Solvent-based protocol: To a solution of N,N′-bis(2-ethylhexyl)-2,6-dibromo-1,4,5,8-naphthalenetetracarboxylic acid bisimide (0.445 mmol, 0.5 equiv.) in

anhydrous toluene (5 mL) were introduced, potassium carbonate (1.338 mmol, 1.5 equiv.); pivalic acid (0.134 mmol, 0.15 equiv.), thiophene (4.46 mmol, 5 equiv.), and palladium(II) acetate (0.004 mmol, 0.005 equiv.). The mixture was left to stir and reflux at 120°C for 18 hours. The reaction mixture was left to cool down at room temperature then filtered over celite. The dark red solution was poured over brine (50 mL), extracted with ethyl acetate (3 x 50 mL), dried with magnesium sulphate, filtered, and concentrated by rotating evaporator to afford a dark red product. The crude product was purified on silica gel (dichloromethane/hexane 1:1) to afford the desired product as a dark red solid. **^{1}H NMR** (600 MHz, chloroform-d) δ = 8.76 (s, 2H, H$_{arom.}$), 7.57 (dd, 2H, J = 5.1, 1.2 Hz, H$_{thioph.}$), 7.30 (dd, 2H, J = 3.5, 1.2 Hz, H$_{thioph.}$), 7.20 (td, 2H, J = 5.1, 3.5 Hz, H$_{thioph.}$), 4.09–4.06 (m, 4H, R-CH$_2$-CH-(CH$_2$)$_n$-CH$_3$), 1.92–1.89 (m, 2H, R-CH$_2$-CH-(CH$_2$)$_n$-CH$_3$), 1.37–1.24 (m, 16H, R-CH$_2$-CH-(CH$_2$)$_n$-CH$_3$), 0.91–0.85 (m, 12H, R-CH$_2$-CH-(CH$_2$)$_n$-CH$_3$).

2,6-diphenyl-pyrrolo[3,4-f]isoindole-1,3,5,7-tetraone
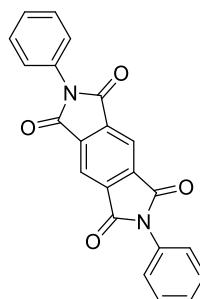
Solvent-based protocol: To a solution of pyromellitic dianhydride (870.7 mg, 3.99 mmol, 1 equiv.) in dry DMF (10 mL) was added aniline (929.3 mg, 0.91 mL, 9.98 mmol, 2.5 equiv.) with a syringe over a period of 3 minutes. The resulting mixture was stirred at reflux for 2 hours under argon atmosphere. The reaction mixture was cooled to room temperature and the resulting precipitate was filtered, washed with methanol, and dried overnight in vacuum oven to afford the desired product as pale-yellow crystals (1.164 g, 79%). The crude product was used without further purification and purity determined by elemental analysis only as the crystals showed no solubility in any usual solvent. **MS** (EI) – (m/z) for C$_{22}$H$_{12}$N$_2$O$_4$ calc. 368; found 368. **MP**: >400°C. **EA** for C$_{22}$H$_{12}$N$_2$O$_4$ calc. C, 71.74; H, 3.28; N, 7.61; found C, 71.67; H, 3.19; N, 7.63.

2,6-dibenzylpyrrolo[3,4-f]isoindole-1,3,5,7(2H,6H)-tetraone
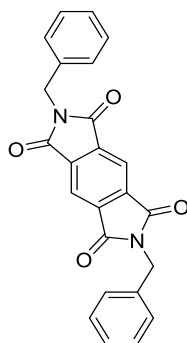
Solvent-based protocol: To a solution of pyromellitic dianhydride (606.4 mg, 2.78 mmol, 1 equiv.) in acetic acid (10 mL) was added benzylamine (893.6 mg, 0.91 mL, 8.34 mmol, 3 equiv.) with a syringe in one portion. The resulting mixture was stirred at reflux for 3 hours. The reaction mixture was poured over ice and water and the resulting pinkish precipitate was filtered and washed with ethanol to afford a colourless solid. The crude product was recrystallized from ethanol to afford the desired product as colourless crystals (462.9 mg, 42%). **^{1}H NMR** (600 MHz, chloroform-d) δ = 8.26 (s, 2H, H$_{arom.}$), 7.44 (d, 4H, J = 7.2 Hz, H$_{Ph}$), 7.33 (t, 4H, J = 8.3, 6.6 Hz, H$_{Ph}$), 7.29 (t, 2H, H$_{Ph}$), 4.89 (s, 4H, R-CH$_2$- Ph). **MS** (EI) – (m/z) for $C_{24}H_{16}N_2O_4$ calc. 396; found 396. **MP**: 302-303°C. **EA** for $C_{24}H_{16}N_2O_4$ calc. C, 72.72; H, 4.07; N, 7.07; found C, 72.63; H, 4.18; N, 7.11.

Solid-state protocol: In one step, pyromellitic dianhydride (249.5 mg, 1.14 mmol, 1 equiv.), benzylamine (306.4 mg, 312.3 μL, 2.86 mmol, 2.5 equiv.), and acetic acid (167 μL) were introduced in a 50 mL stainless steel grinding jar with 8 stainless steel balls (12 mm diameter). Total mass of the reagents was calculated so that milling load equals 13 mg.mL^{-1}. The jar was closed and subjected to grinding for 90 minutes in the VBM operated at 30 Hz. The resulting pale blue slurry was collected with the minimum amount of dichloromethane, filtered over celite and the filtrate concentrated by rotary evaporation to afford a colourless solid. The crude product was recrystallized from ethanol to afford colourless solid (86.2 mg, 19%).

5. REFERENCES AND NOTES

1 L. Panther, D. Guest, A. McGown, H. Emerit, R. Tareque, A. Jose, chris M. dadswell, simon coles, G. Tizzard, R. Gonzalez-Mendez, C. Goodall, M. Bagley, J. Spencer and B. W. Greenland, *Chemistry – A European Journal*, , DOI:https://doi.org/10.1002/chem.202201444.

2 Y. N. Harari, D. Vandermeulen and D. Casanave, *Sapiens: A Graphic History*, HarperCollins, 2020.

3 P. T. Anastas and J. Charles. Warner, *Green chemistry : theory and practice*, Oxford University Press, Oxford [England]; New York, 1998.

4 J. Britton and C. L. Raston, *Chemical Society Reviews*, 2017, **46**, 1250–1271.

5 S. V. Ley and I. R. Baxendale, *Chimia (Aarau)*, 2008, **62**, 162–168.

6 A. J. Close, P. Kemmitt, M. K. Emmerson and J. Spencer, *Tetrahedron*, 2014, **70**, 9125–9131.

7 C. O. Kappe, *Comprehensive Medicinal Chemistry II*, 2006, **3**, 837–860.

8 M. Panunzio, E. Campana, G. Martelli, P. Vicennati and E. Tamanini, *Materials Research Innovations*, 2004, **8**, 27–31.

9 K. Itho, M. Sumimoto and H. Tanaka, *Journal of Wood Chemistry and Technology*, 1993, **13**, 463–479.

10 S. L. James, C. J. Adams, C. Bolm, D. Braga, P. Collier, T. Friščić, F. Grepioni, K. D. M. Harris, G. Hyett, W. Jones, A. Krebs, J. Mack, L. Maini, A. G. Orpen, I. P. Parkin, W. C. Shearouse, J. W. Steed and D. C. Waddell, *Chem. Soc. Rev*, 2012, **41**, 413–447.

11 A. L. Garay, A. Pichon and S. L. James, *Chemical Society Reviews*, 2007, **36**, 846–855.

12 N. R. Rightmire and T. P. Hanusa, *Dalton Transactions*, 2016, **45**, 2352–2362.

13 G. A. Bowmaker, *Chemical Communications*, 2013, **49**, 334–348.

14 L. Takacs, *Chemical Society Reviews*, 2013, **42**, 7649–7659.

15 J. G. Hernández and C. Bolm, *Journal of Organic Chemistry*, 2017, **82**, 4007–4019.

16 C. Bolm, R. Mocci, C. Schumacher, M. Turberg, F. Puccetti and J. G. Hernández, *Angewandte Chemie - International Edition*, 2018, **57**, 2423–2426.

17 E. Mohammadi, L. Petera, H. Saeidfirozeh, A. Knížek, P. Kubelík, R. Dudžák, M. Krůs, L. Juha, S. Civiš, R. Coulon, O. Malina, J. Ugolotti, V. Ranc, M. Otyepka, J. Šponer, M. Ferus and J. E. Šponer, *Chemistry – A European Journal*, 2020, **26**, 12075–12080.

18 M. Ferguson, M. S. Moyano, G. A. Tribello, D. E. Crawford, E. M. Bringa, S. L. James, J. Kohanoff and M. G. Del Pópolo, *Chemical Science*, 2019, **10**, 2924–2929.

19 B. P. Hutchings, D. E. Crawford, L. Gao, P. Hu and S. L. James, *Angewandte Chemie - International Edition*, 2017, **56**, 15252–15256.

20 X. Ma, W. Yuan, S. E. J. Bell and S. L. James, *Chemical Communications*, 2014, **50**, 1585–1587.

21 Y. S. Kwon, K. B. Gerasimov and S. K. Yoon, *Journal of Alloys and Compounds*, 2002, **346**, 276–281.

22 L. Takacs and J. S. McHenry, *Journal of Materials Science*, 2006, **41**, 5246–5249.

23 J. L. Howard, Q. Cao and D. L. Browne, *Chemical Science*, 2018, **9**, 3080–3094.

24 F. Gomollón-Bel, *Chemistry International*, 2019, **41**, 12–17.

25 Y. Yeboue, B. Gallard, N. Le Moigne, M. Jean, F. Lamaty, J. Martinez and T. X. Métro, *ACS Sustainable Chemistry and Engineering*, 2018, **6**, 16001–16004.

26 P. Simonetti, R. Nazir, A. Gooneie, S. Lehner, M. Jovic, K. A. Salmeia, R. Hufenus, A. Rippl, J. P. Kaiser, C. Hirsch, B. Rubi and S. Gaan, *Composites Part B: Engineering*, 2019, **178**, 107470.

27 H. A. Garekani, A. Nokhodchi, M. A. Rayeni and F. Sadeghi, *Drug Development and Industrial Pharmacy*, 2013, **39**, 1238–1246.

28 H. G. Moradiya, A. Nokhodchi, M. S. A. Bradley, R. Farnish and D. Douroumis, *Pharmaceutical Development and Technology*, 2016, **21**, 445–452.

29 M. Maniruzzaman and A. Nokhodchi, *Drug Discovery Today*, 2017, **22**, 340–351.

30 D. K. Tan, M. Maniruzzaman and A. Nokhodchi, *Pharmaceutics*, 2018, **10**, 203.

31 Q. Cao, D. E. Crawford, C. Shi and S. L. James, *Angewandte Chemie International Edition*, 2020, **59**, 4478–4483.

32 April 25, 1954: Bell Labs Demonstrates the First Practical Silicon Solar Cell, https://www.aps.org/publications/apsnews/200904/physicshistory.cfm.

33 A History of Solar Cells: How Technology Has Evolved, https://www.solarpowerauthority.com/a-history-of-solar-cells/.

34 M. Jeppesen, Solar power in space: 60th anniversary of Vanguard 1, https://reneweconomy.com.au/solar-power-in-space-60th-anniversary-of-vanguard-1-41568/.

35 S. R, K. AA and A. T, *Journal of Material Science & Engineering*, 2017, **06**, 1–16.

36 L. Ma, S. Zhang, J. Wang, Y. Xu and J. Hou, *Chemical Communications*, 2020, **56**, 14337–14352.

37 J. F. Geisz, R. M. France, K. L. Schulte, M. A. Steiner, A. G. Norman, H. L. Guthrey, M. R. Young, T. Song and T. Moriarty, *Nature Energy*, 2020, **5**, 326–335.

38 A. Facchetti, *Materials Today*, 2013, **16**, 123–132.

39 J. J. M. Halls, C. A. Walsh, N. C. Greenham, E. A. Marseglia, R. H. Friend, S. C. Moratti and A. B. Holmes, *Nature*, 1995, **376**, 498–500.

40 G. Yu and A. J. Heeger, *Journal of Applied Physics*, 1995, **78**, 4510–4515.

41   R. Taylor, J. P. Hare, A. K. Abdul-Sada and H. W. Kroto, *Journal of the Chemical Society, Chemical Communications*, 1990, 1423–1425.

42   J. C. Hummelen, B. W. Knight, F. Lepeq, F. Wudl, J. Yao and C. L. Wilkins, *Journal of Organic Chemistry*, 1995, **60**, 532–538.

43   M. M. Wienk, J. M. Kroon, W. J. H. Verhees, J. Knol, J. C. Hummelen, P. A. Van Hal and R. A. J. Janssen, *Angewandte Chemie - International Edition*, 2003, **42**, 3371–3375.

44   H. Y. Chen, J. Hou, S. Zhang, Y. Liang, G. Yang, Y. Yang, L. Yu, Y. Wu and G. Li, *Nature Photonics*, 2009, **3**, 649–653.

45   Y. Liang, Y. Wu, D. Feng, S. T. Tsai, H. J. Son, G. Li and L. Yu, *J Am Chem Soc*, 2009, **131**, 56–57.

46   Y. Liang and L. Yu, *Accounts of Chemical Research*, 2010, **43**, 1227–1236.

47   Y. Li, *Accounts of Chemical Research*, 2012, **45**, 723–733.

48   S. H. Liao, H. J. Jhuo, Y. S. Cheng and S. A. Chen, *Advanced Materials*, 2013, **25**, 4766–4771.

49   M. Li, K. Gao, X. Wan, Q. Zhang, B. Kan, R. Xia, F. Liu, X. Yang, H. Feng, W. Ni, Y. Wang, J. Peng, H. Zhang, Z. Liang, H. L. Yip, X. Peng, Y. Cao and Y. Chen, *Nature Photonics*, 2017, **11**, 85–90.

50   Y. Chen, X. Wan and G. Long, *Accounts of Chemical Research*, 2013, **46**, 2645–2655.

51   J. Zhao, Y. Li, G. Yang, K. Jiang, H. Lin, H. Ade, W. Ma and H. Yan, *Nature Energy*, 2016, **1**, 15027.

52   Y. He and Y. Li, *Physical Chemistry Chemical Physics*, 2011, **13**, 1970–1983.

53   Y. He, H. Y. Chen, J. Hou and Y. Li, *J Am Chem Soc*, 2010, **132**, 1377–1382.

54   P. Cheng and X. Zhan, *Chemical Society Reviews*, 2016, **45**, 2544–2582.

55   K. D. Deshmukh, T. Qin, J. K. Gallaher, A. C. Y. Liu, E. Gann, K. O'Donnell, L. Thomsen, J. M. Hodgkiss, S. E. Watkins and C. R. McNeill, *Energy and Environmental Science*, 2015, **8**, 332–342.

56   C. W. Tang, *Applied Physics Letters*, 1986, **48**, 183–185.

57   C. Yan, S. Barlow, Z. Wang, H. Yan, A. K.-Y. Jen, S. R. Marder and X. Zhan, *Nature Reviews Materials*, 2018, **3**, 18003.

58   Y. Lin and X. Zhan, *Advanced Energy Materials*, 2015, **5**, 1–9.

59   R. Ma, T. Liu, Z. Luo, K. Gao, K. Chen, G. Zhang, W. Gao, Y. Xiao, T. K. Lau, Q. Fan, Y. Chen, L. K. Ma, H. Sun, G. Cai, T. Yang, X. Lu, E. Wang, C. Yang, A. K. Y. Jen and H. Yan, *ACS Energy Letters*, 2020, **5**, 2711–2720.

60   Computational Database for Active Layer Materials for Organic Photovoltaic Solar Cells, https://organicelectronics.nrel.gov/.

61   Q. Li, M. Peng, H. Li, C. Zhong, L. Zhang, X. Cheng, X. Peng, Q. Wang, J. Qin and Z. Li, *Organic Letters*, 2012, **14**, 2094–2097.

62   R. Haldar, A. Mazel, R. Joseph, M. Adams, I. A. Howard, B. S. Richards, M. Tsotsalas, E. Redel, S. Diring, F. Odobel and C. Wöll, *Chemistry - A European Journal*, 2017, **23**, 14316–14322.

63   F. S. Etheridge, R. Fernando, J. A. Golen, A. L. Rheingold and G. Sauve, *RSC Advances*, 2015, **5**, 46534–46539.

64   F. Doria, M. Nadai, M. Folini, M. Di Antonio, L. Germani, C. Percivalle, C. Sissi, N. Zaffaroni, S. Alcaro, A. Artese, S. N. Richter and M. Freccero, *Organic and Biomolecular Chemistry*, 2012, **10**, 2798–2806.

65   F. Chaignon, M. Falkenström, S. Karlsson, E. Blart, F. Odobel and L. Hammarström, *Chemical Communications*, 2007, 64–66.

66   A. Sarkar, S. Dhiman, A. Chalishazar and S. J. George, *Angewandte Chemie - International Edition*, 2017, **56**, 13767–13771.

67   S. Kuila, K. V. Rao, S. Garain, P. K. Samanta, S. Das, S. K. Pati, M. Eswaramoorthy and S. J. George, *Angewandte Chemie - International Edition*, 2018, **57**, 17115–17119.

68   S. Valero, A. Cabrera-Espinoza, S. Collavini, J. Pascual, N. Marinova, I. Kosta and J. L. Delgado, *European Journal of Organic Chemistry*, 2020, **2020**, 5329–5339.

69   S. Guo, W. Wu, H. Guo and J. Zhao, *Journal of Organic Chemistry*, 2012, **77**, 3933–3943.

70   S. Guo, J. Sun, L. Ma, W. You, P. Yang and J. Zhao, *Dyes and Pigments*, 2013, **96**, 449–458.

71   P. Wang, H. Li, C. Gu, H. Dong, Z. Xu and H. Fu, *RSC Advances*, 2015, **5**, 19520–19527.

72   Y. An, X. Xu, K. Liu, X. An, C. Shang, G. Wang, T. Liu, H. Li, H. Peng and Y. Fang, *Chemical Communications*, 2019, **55**, 941–944.

73   Z. Chen, Y. Zheng, H. Yan and A. Facchetti, *J Am Chem Soc*, 2009, **131**, 8–9.

74   H. Shokouhi Mehr, N. C. Romano, R. Altamimi, J. M. Modarelli and D. A. Modarelli, *Dalton Transactions*, 2015, **44**, 3176–3184.

75   L. Liu, S. Guo, J. Ma, K. Xu, J. Zhao and T. Zhang, *Chemistry - A European Journal*, 2014, **20**, 14282–14295.

76   A. T. Pham and S. Matile, *Chemistry - An Asian Journal*, 2020, **15**, 1562–1566.

77   Y. V. Suseela, M. Sasikumar and T. Govindaraju, *Tetrahedron Letters*, 2013, **54**, 6314–6318.

78   T. D. M. Bell, S. Yap, C. H. Jani, S. V. Bhosale, J. Hofkens, F. C. D. Schryver, S. J. Langford and K. P. Ghiggino, *Chemistry - An Asian Journal*, 2009, **4**, 1542–1550.

79   A. A. Berezin, A. Sciutto, N. Demitri and D. Bonifazi, *Organic Letters*, 2015, **17**, 1870–1873.

80   S. Hernández, C. Ottone, S. Proto, K. Tolod, M. Díaz De Los Bernardos, A. Solé-Daura, J. J. Carbó, C. Godard, S. Castillón, N. Russo, G. Saracco and C. Claver, *Green Chemistry*, 2017, **19**, 2448–2462.

81   A. A. Ahmed, R. Angell, S. Oxenford, J. Worthington, N. Williams, N. Barton, T. G. Fowler, D. E. O'Flynn, M. Sunose, M. McConville, T. Vo,
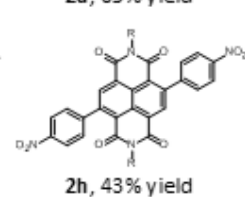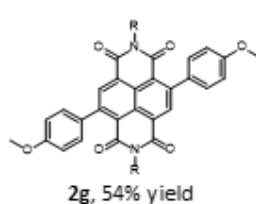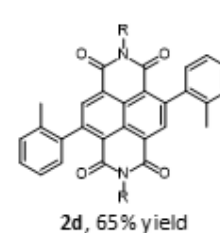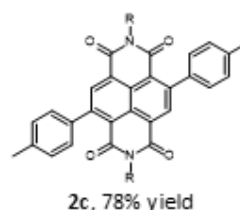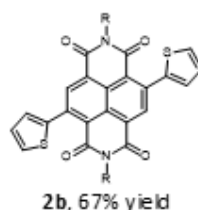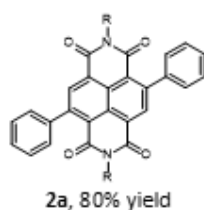
W. D. Wilson, S. A. Karim, J. P. Morton and S. Neidle, *ACS Medicinal Chemistry Letters*, 2020, **11**, 1634–1644.

82   Y. Liu, W. Wu, J. Zhao, X. Zhang and H. Guo, *Dalton Transactions*, 2011, **40**, 9085–9089.

83   B. C. Popere, A. M. Della Pelle and S. Thayumanavan, *Macromolecules*, 2011, **44**, 4767–4776.

84   S. Wu, F. Zhong, J. Zhao, S. Guo, W. Yang and T. Fyles, *Journal of Physical Chemistry A*, 2015, **119**, 4787–4799.

85   M. Hussain, M. Taddei, L. Bussotti, P. Foggi, J. Zhao, Q. Liu and M. Di Donato, *Chemistry - A European Journal*, 2019, **25**, 15615–15627.

86   K. Chen, J. Zhao, X. Li and G. G. Gurzadyan, *Journal of Physical Chemistry A*, 2019, **123**, 2503–2516.

87   Z. Yuan, Y. Ma, T. Geßner, M. Li, L. Chen, M. Eustachi, R. T. Weitz, C. Li and K. Müllen, *Organic Letters*, 2016, **18**, 456–459.

88   H. F. Higginbotham, S. Maniam, S. J. Langford and T. D. M. Bell, *Dyes and Pigments*, 2015, **112**, 290–297.

89   S. V. Bhosale, M. B. Kalyankar, S. V. Bhosale, S. J. Langford, E. F. Reid and C. F. Hogan, *New Journal of Chemistry*, 2009, **33**, 2409–2413.

90   S. Kuila, A. Ghorai, P. K. Samanta, R. B. K. Siram, S. K. Pati, K. S. Narayan and S. J. George, *Chemistry - A European Journal*, 2019, **25**, 16007–16011.

91   K. Mandal, D. Bansal, Y. Kumar, Rustam, J. Shukla and P. Mukhopadhyay, *Chemistry - A European Journal*, 2020, **26**, 10607–10619.

92   S. Maniam, R. P. Cox, S. J. Langford and T. D. M. Bell, *Chemistry - A European Journal*, 2014, **21**, 4133–4140.

93   R. E. Dawson, A. Hennig, D. P. Weimann, D. Emery, V. Ravikumar, J. Montenegro, T. Takeuchi, S. Gabutti, M. Mayor, J. Mareda, C. A. Schalley and S. Matile, *Nature Chemistry*, 2010, **2**, 533–538.

94 V. Figà, C. Chiappara, F. Ferrante, M. P. Casaletto, F. Principato, S. Cataldo, Z. Chen, H. Usta, A. Facchetti and B. Pignataro, *Journal of Materials Chemistry C*, 2015, **3**, 5985–5994.

95 C. Gu, W. Hu, J. Yao and H. Fu, *Chemistry of Materials*, 2013, **25**, 2178–2183.

96 R. Matsidik, H. Komber, A. Luzio, M. Caironi and M. Sommer, *J Am Chem Soc*, 2015, **137**, 6705–6711.

97 T. Seo, T. Ishiyama, K. Kubota and H. Ito, *Chemical Science*, 2019, **10**, 8202–8210.

98 S. Amemori, K. Kokado and K. Sada, *Angewandte Chemie - International Edition*, 2013, **52**, 4174–4178.

99 R. Schmidt, H. Martin Scholze and A. Stolle, *International Journal of Industrial Chemistry*, 2016, **7**, 181–186.

100 N. Cindro, M. Tireli, B. Karadeniz, T. Mrla and K. Užarević, *ACS Sustainable Chemistry and Engineering*, 2019, **7**, 16301–16309.

101 M. Sasikumar, Y. V. Suseela and T. Govindaraju, *Asian Journal of Organic Chemistry*, 2013, **2**, 779–785.

102 X. Guo and M. D. Watson, *Organic Letters*, 2008, **10**, 5333–5336.

103 S. Sato, A. Kajima, H. Hamanaka and S. Takenaka, *Journal of Organometallic Chemistry*, 2019, **897**, 107–113.

104 F. Cuenca, O. Greciano, M. Gunaratnam, S. Haider, D. Munnur, R. Nanjunda, W. D. Wilson and S. Neidle, *Bioorganic and Medicinal Chemistry Letters*, 2008, **18**, 1668–1673.

105 C. D. Smith, R. C. Bott, S. E. Bottle, A. S. Micallef and G. Smith, *Journal of the Chemical Society, Perkin Transactions 2*, 2002, 533–537.

106 G. Ding, X. Wu, B. Lu, W. Lu, Z. Zhang and X. Xie, *Tetrahedron*, 2018, **74**, 1144–1150.

107 A. Magyarosy, R. M. Mohareb and J. Z. Ho, *Heteroatom Chemistry*, 2006, **17**, 648–652.

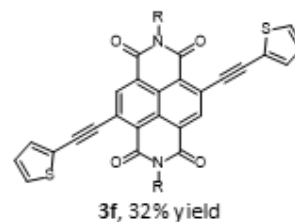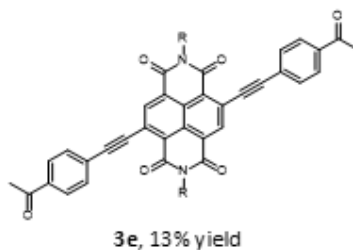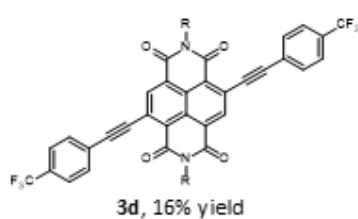108 T. Gensch, M. N. Hopkinson, F. Glorius and J. Wencel-Delord, *Chemical Society Reviews*, 2016, **45**, 2900–2936.
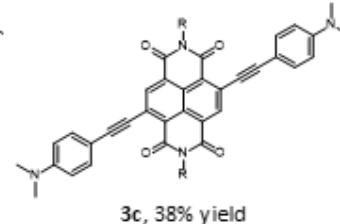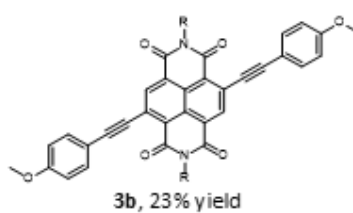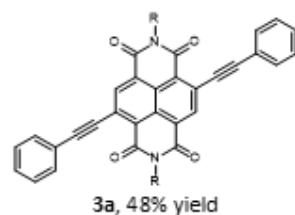
109 H. Bohra and M. Wang, *Journal of Materials Chemistry A*, 2017, **5**, 11550–11571.

110 J. G. Hernández, *Chemistry - A European Journal*, 2017, **23**, 17157–17165.

111 S. J. Lou, Y. J. Mao, D. Q. Xu, J. Q. He, Q. Chen and Z. Y. Xu, *ACS Catalysis*, 2016, **6**, 3890–3894.

112 S. Zhao, Y. Li, C. Liu and Y. Zhao, *Tetrahedron Letters*, 2018, **59**, 317–324.

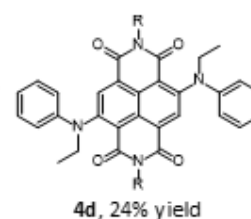113 P. Anastas and N. Eghbali, *Chemical Society Reviews*, 2010, **39**, 301–312.
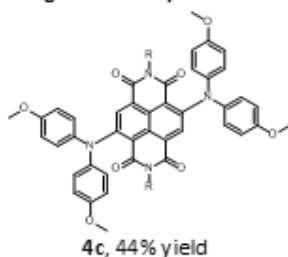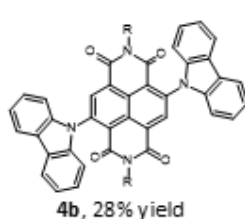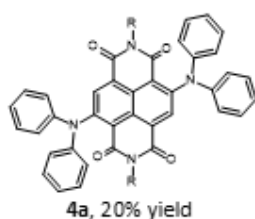
6. APPENDIX

Scope of Suzuki-Miyaura coupled products

2a, 80% yield

2b, 67% yield

2c, 78% yield

2d, 65% yield

2e, 83% yield

2f, 59% yield

2g, 54% yield

2h, 43% yield

2i, XX% yield

2j, XX% yield
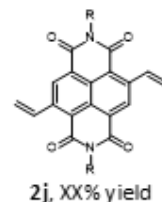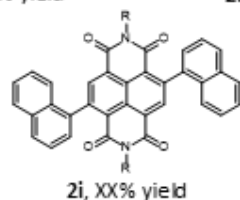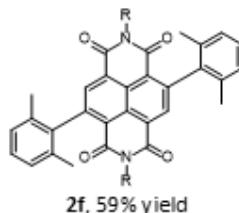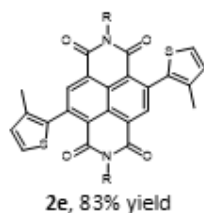
Scope of Sonogashira coupled products

3a, 48% yield

3b, 23% yield

3c, 38% yield

3d, 16% yield

3e, 13% yield

3f, 32% yield

Scope of Buchwald-Hartwig amination products

4a, 20% yield

4b, 28% yield

4c, 44% yield

4d, 24% yield

Appendix 1. Compounds isolated by solid state reactions by Lydia Pearce few months after the work from this report.

---

[i] In case of liquid-assisted grinding (LAG) which is defined as the mechanical reduction of the particle size of a solid sample by attribution (friction), impact or cutting in the presence of a small amount of solvent. This introduced the parameter η, defined as the ratio of the added liquid (in µL) to the total weight of the solid reactants (in mg), replacing vaguer terms such as "a few drops of liquid" or "small amount of liquid". It is empirically found to be in the range of ca. 0-1 µL.mg^{-1}. In this study, η = 1 µL.mg^{-1}.

[ii] Defined as the weight of grinding stock divided by the free volume in the grinding jar. Its value is most of the time between 5 and 40 mg.mL^{-1}.